EPA-650/2-74-036

May 1974

Environmental Protection Technology Series

BRAXTON SONIC AGGLOMERATOR EVALUATION

Office of Research and Development
U.S. Environmental Protection Agency
Washington, DC 20460

EPA-650/2-74-036

BRAXTON SONIC AGGLOMERATOR EVALUATION

by

Richard Dennis, Robert Bradway,
and Reed Cass

GCA Corporation
GCA/Technology Division
Bedford, Massachusetts 01730

Contract No. 68-02-1316 (Task 1)
ROAP No. 21ADL-04
Program Element No. 1AB012

EPA Task Officer: Dale Harmon

Control Systems Laboratory
National Environmental Research Center
Research Triangle Park, North Carolina 27711

Prepared for

OFFICE OF RESEARCH AND DEVELOPMENT
U.S. ENVIRONMENTAL PROTECTION AGENCY
WASHINGTON, D.C. 20460

May 1974

This report has been reviewed by the Environmental Protection Agency and approved for publication. Approval does not signify that the contents necessarily reflect the views and policies of the Agency, nor does mention of trade names or commercial products constitute endorsement or recommendation for use.

ABSTRACT

This report presents the evaluation of a novel air pollution control system developed by the Braxton Corporation. The alternating velocity precipitator, or sonic agglomerator, is designed to decrease the number and increase the size of particles in a gas stream by agglomeration induced by a standing sound wave through which the aerosol moves. A prototype unit of the alternating velocity precipitator was tested to determine its basic performance characteristics and to evaluate the effect of the addition of water and/or steam to the system's performance.

Results from those tests using resuspended cupola dust indicate that the device decreases the mass of fine particles but that the reduction is more highly correlated to the use of water sprays than to the use of the sonic generator. The correlation coefficients relating the use of sound and water sprays to fine particle reduction are statistically significant but the correlation coefficient for steam addition is not statistically significant.

The particle size distributions of the fine particles at both the inlet and outlet of the sonic agglomerator were determined with Andersen cascade impactors. Although shifts between the inlet and outlet size distributions were often observed, there was no clear trend to the changes and they could not be correlated to system operating parameters.

CONTENTS

FIGURES

FIGURES (continued)

TABLES

ACKNOWLEDGMENTS

The information and support provided by Mr. Ed Kent and the Braxton staff are acknowledged with sincere thanks.

SECTION I

CONCLUSIONS

The prototype sonic agglomerator tested in this program collected 42 to 59 percent of the test dust entering it without the use of sound, water or steam. The collection efficiencies using resuspended cupola dust and different combinations of sound, steam and water ranged from 81 to 97 percent. These efficiencies are based on using a cyclone after the sonic agglomerator equal in collection efficiency to the cyclone used for sampling during these tests.

The amount of fine particles, as defined by the cyclone undersize dust (less than about 2 μm), was measured upstream and downstream of the chamber and the use of sound and water sprays reduced the fine fraction at the outlet. The reduction in fine particles as a result of conditioning by the sonic agglomerator system under various operating modes ranged from 14 to 83 percent.

The correlation coefficients for the small particle reduction for all test runs with sound, water and steam individually and neglecting other operating parameters were 0.68, 0.65 and 0.06 respectively. The coefficients for sound and water are statistically significant while that for steam is not. A multiple regression analysis of those tests using cupola dust shows that the use of steam is not significant but that the use of water sprays and the sonic generator are highly significant in reducing the mass of fine particles. The regression analysis also shows that the sonic generator has less influence on fine particle reduction than does water sprays when using resuspended cupola dust.

Cascade impactor samples of the cyclone undersize material at the inlet and outlet of the unit showed no consistent trend in the shift of particle size distributions. Some tests resulted in an outlet dust with a larger mass median diameter than the inlet dust, others resulted in an outlet dust with a smaller mass median diameter than the inlet, and some tests showed no change. These results do not appear to correlate with any system operating parameters.

The estimated annual operating costs for the sonic agglomerator system using sound and water is $13.30/m^3/minute ($0.38/cfm). The use of a nominal amount of steam in addition to sound and water results in an annual operating cost of $46.22/m^3/minute ($1.32/cfm). These estimates are based upon the costs of 1,000/m^3/minute (35,000 cfm) unit and do not include any annualized capital costs.

SECTION II

RECOMMENDATIONS

This program was limited to the field evaluation as described in this report. It was not within the scope of the program to make specific recommendations concerning the sonic agglomerator system design or ultimate use. It is recommended, however, that if the alternating velocity precipitator is to become a viable part of an industrial gas cleaning system, then the several operating parameters must be optimized. The use of steam should be reexamined and the optimum interaction of sound and water sprays should be determined. In an industrial sized unit the ultimate disposal or reuse of the effluent base wash that contains whatever dust is retained in the chamber must also be examined.

SECTION III

INTRODUCTION

The purpose of this study was to determine the basic performance characteristics of a sonic agglomerator that was designed and constructed by the Braxton Corporation. All tests were performed on a prototype unit at the Braxton plant in Medfield, Massachusetts.

The sonic agglomerator, or alternating velocity precipitator (AVP), is designed to impart different velocities to particles of different sizes, hence increasing the probability of collisions that result in agglomeration. When sufficient coagulation occurs, the number of small particles is decreased through collisions with larger ones creating a dust of large enough particle size to be capable of being efficiently collected by a low energy gas cleaning device such as a cyclone. A more detailed discussion of the theoretical basis of acoustic coagulation is presented in Appendix A.

Since the agglomeration rate should be enhanced by both a higher concentration and wider size range of the inlet particulate, the system is designed to allow the admission of steam and/or water droplets. The steam can be added in the acoustical chamber or, as was done in those tests in which steam was used in this study, added in the inlet duct about 50 feet before the chamber. This allows the dust and steam to interact, hopefully increasing the cohesive properties of the dust and also raising the humidity of the gas to a point where the liquid particles in the chamber will be preserved. The water is added as a spray at the top of the chamber via Sonicore nozzles. According to the manufacturer the Sonicore nozzles deliver a spray in the 10-20 μm range.

The chamber itself is approximately 0.75 meter (2.5 feet) in diameter and 4.27 meters (14 feet) in length. The chamber length is adjustable to enable tuning the standing sound wave which is 4-1/2 wave lengths long, so that nodes are located at top and bottom. The sound wave is generated by an electromagnetically driven piston which displaces about $\pm$ 0.05 cm. ($\pm$ 0.02 inches) at a frequency of 366 Hz. The sound intensity inside the

chamber is 165 decibels. Any material that is precipitated from the gas stream before exiting the chamber is washed off the base plate and out of the system with a continuous flow of water.

The prototype unit tested was designed for a maximum flow rate of 7.0 m^3/s (15,000 cfm). Existing fan capabilities limited the flow to 3.7 m^3/s (8,000 cfm) but most tests were run at 2.2 m^3/s (5,000 cfm). At the latter flow rate the average velocity in the chamber was 5.2 m/s (1,030 feet per minute) while at the inlet and outlet ducts (2 foot diameter) the average velocity was 8.1 m/s (1,600 feet per minute).

There are several factors that could lead to particulate depletion in the system besides the agglomeration and subsequent fallout as a result of sonic action. For example, there could be wash out from the water spray system, the larger fraction entering the chamber may settle without further coagulation because of the relatively low velocity in the chamber, or the right angle bends at the entrance and exit of the chamber may remove some particulate. The test program was designed in such a way as to first establish the effectiveness of the entire system and then determine the role of each of the components (sound, steam, water, velocity, etc.).

SECTION IV

SAMPLING METHODS

The sonic agglomerator is designed to increase the size of small particles and, as such, is a preconditioner rather than a collector. Although some dust would be expected to remain in the sonic chamber, the effectiveness of the device can be determined only by characterizing the properties of the outlet dust that would make it more readily collectable than the inlet dust. Since the Braxton system is designed to be followed by a cyclone as a final collector, a sampling system with a cyclone followed by a filter would allow determination of the change in mass of the cyclone undersize material as a result of the conditioning system.

To further characterize the effectiveness of the system, cascade impactor samples were taken of the cyclone undersize material at both the inlet and outlet. This showed any shifts in the particle size distribution of the fine material.

The sampling system used in this study is shown schematically in Figure 1 and calibrations for specific components are detailed in Appendix B. A portion of the system flow was withdrawn isokinetically through a sampling nozzle (a). The nozzles were interchangeable and a set was designed and manufactured to match all flow combinations used during the tests. The sampled gas stream then entered the probe (b) connecting the nozzle and the cyclone. This probe was one inch copper pipe and the bend before the cyclone was necessitated by space limitations at the prototype unit. The larger sized dust fraction was then separated by an Aerotec model 1½ cyclone (c) manufactured by UOP Air Correction. The cyclone was also used to meter the flow in the sampling system by measuring the pressure drop across it with a manometer (d). A variable transformer on the main sampling pump was used to maintain 746.5 $n/_m 2$ (3 inches water) differential across the cyclone which corresponded to 0.0085 $m^3/_s$ (18 cfm).

The exit duct from the cyclone (e) was also one inch copper pipe with a small port drilled in it about twenty duct diameters downstream. This

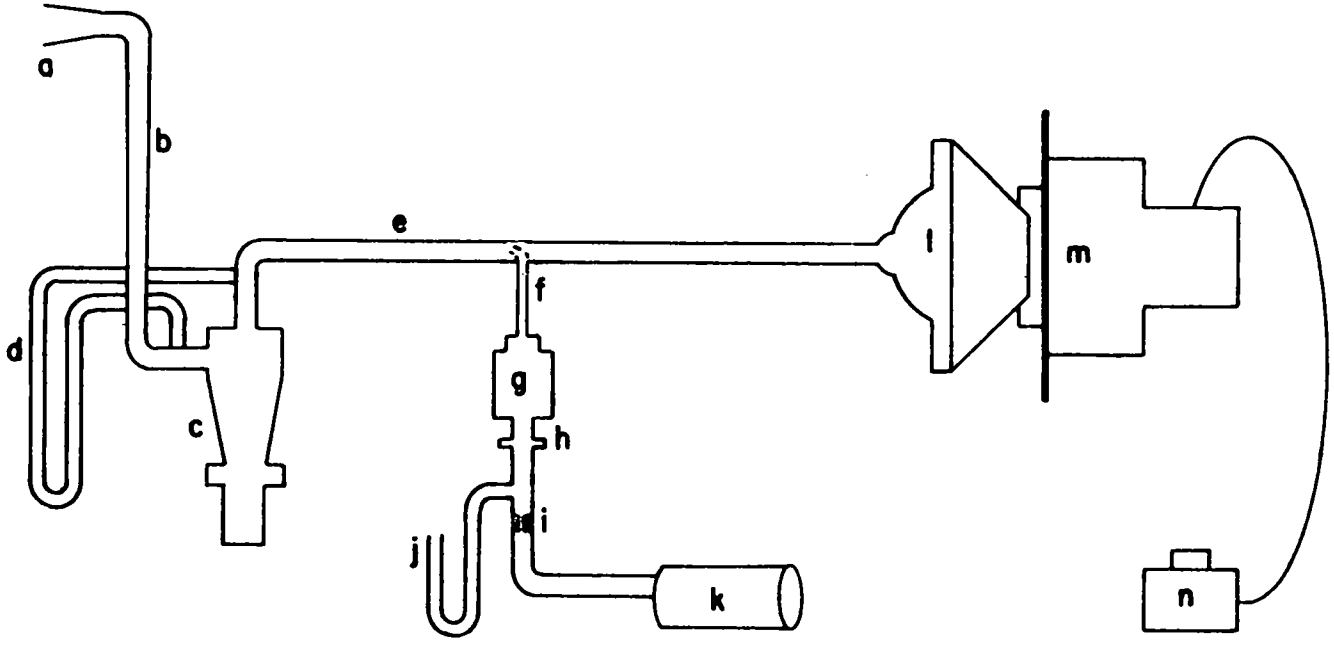

Figure 1. Schematic of Sampling Train

allowed access for the small probe (f) which led to the Andersen six stage cascade impactor (g). The probe was designed for isokinetic sampling and kept as short as possible. The collection surfaces of the cascade impactors were coated before use with a thin uniform layer of petroleum jelly to minimize particle bounce and reintrainment. The impactor was followed by a glass fiber filter (h) and a critical orifice (i) for flow control. Conditions for critical flow were monitored by observing the upstream pressure with a mercury manometer (j) and knowing the pump pressure capabilities of the model 0522-V3-G18D Gast pump (k). Laboratory measurements determined that the Gast pumps used were capable of maintaining a flow rate of one cubic foot per minute at an absolute suction pressure of 10.2 inches of mercury. Since critical flow of air through an orifice is achieved when the pressure downstream of the orifice is less than or equal to 0.53 of the upstream pressure, a downstream absolute pressure of 10.2 inches of mercury assures that critical flow will occur if the upstream absolute pressure is 19.25 inches of mercury or more. Monitoring the upstream pressure also allowed the critical flowrate to be corrected to standard conditions.

The cyclone undersize dust that was not diverted through the impactor continued on to a glass fiber filter (l). The filter holder was a Precision Scientific model high volume sampler (m) with the inlet modified to make a smooth transition from the copper pipe to the filter area. The high volume sampler was the main air mover of the sampling system and the flow rate through it was controlled electrically by a variable transformer (n) so that the pressure drop across the cyclone remained constant.

The resistance across the high volume filter increased quite rapidly and it was found that fifteen minutes was a safe sampling time without overextending the capabilities of the high volume sampler. It also became apparent after the first few runs that the dust concentration was apt to fluctuate with time so that it was very important to have simultaneous upstream and downstream sampling.

An Acrison 120 D dust feeder delivered the test dust to an air ejector which dispersed the dust into the gas stream. Occasionally the dust in the hopper adhered to the side walls, creating a temporary light dust loading in the system. During one test the delivery auger on the feeder broke and

no dust was dispersed at all. Except for that one test, however, the variations in dust concentration due to the dust feeder were minimized, if not eliminated, by simultaneous upstream and downstream sampling.

During some of the first few tests, an attempt was made to traverse the inlet and outlet ducts, sampling at several points in the cross section. The severe space limitations at the sampling locations made this a very awkward procedure. Furthermore, the sampling time restriction of fifteen minutes per filter necessitated disassembling the train and changing the filter in the middle of each run if meaningful traverses were to be made. It was felt that since the sampling ports were installed at locations where velocity and concentration gradients were expected to be minimized, centerline sampling would give meaningful results. Velocity traverses indicated a smooth flow profile and traverses with an Ikor continuous particle monitor showed no large concentration gradients. The Ikor device does not measure the mass concentration directly but measures the electron charge transfer, or triboelectric effect, to monitor particulate concentrations. Measurements with this device at the inlet of the Braxton AVP indicated concentration variations of less than 25 percent across the duct and most of those variations were thought to reflect a temporal variation of dust loading rather than a spatial variation.

SECTION V

ANALYSIS METHODS

After each test run, both the inlet and outlet sampling trains were disassembled and removed to a clean work area. Any dust deposited on the inside of the nozzle and probe before the cyclone was brushed into a tared container. The final net weight of this dust was added to the cyclone catch. The cyclones were stoppered and taken back to the laboratory for cleaning. This was necessitated by the very laborious procedures required to quantitatively remove the dust that did not fall into the hopper but was impinged on the inside of the cyclone.

Any dust deposited on the duct between the cyclone and the high volume sampler was also brushed into a preweighed container and later added to the filter catch. Occasionally some particulates deposited on the walls of the impactor sampling probe. When this occured the dust was added to the first stage of the impactor.

All samples were equilibrated in an atmosphere of less than 50 percent relative humidity at about 65 degrees before weighing. All weighings were done on a Mettler H-15 balance and recorded to the nearest tenth of a milligram.

Sonic agglomerator system parameters such as steam flow rate, water flow rate, sound intensity and power consumption by the sonic generator were recorded by the Braxton personnel operating the unit.

SECTION VI

RESULTS

This section summarizes the results of the test program. Many sonic agglomerator operating parameters were varied during the evaluation procedure and the effects of these variations were assessed by measuring several properties of the inlet and outlet aerosols. The complete matrix of operating variables and dust properties is too vast to present as one unit so the data have been divided into separate sections.

The first section details the system operating parameters such as volume flow rate, sound intensity, rate of steam and water addition and pressure drop across the unit. The next section summarizes the inlet and outlet dust loadings in terms of total mass, cyclone fraction, reduction of total mass, reduction in mass of fine particles and the total system efficiency if a cyclone were to follow the sonic device. The third section shows the changes in the particle size distribution of the fine particles. This is done to show what changes, if any, were imparted to that portion of the dust that penetrated the cyclone collector. The last section is an estimate of operating costs of a 1000 m^3/min. (35,000 cfm) unit if it were to display the same operating characteristics as the prototype unit.

A. SYSTEM OPERATING PARAMETERS

Table 1 details the several sonic agglomerator system operating parameters that were varied during the test program. Most tests were run in the 2 m^3/s (5000 cfm) range as that was considered nominal for the prototype device. Redispersed cupola dust and fly ash were used as test dusts. The cupola dust was used more than the fly ash because the high degree of sphericity and possible poor wetting properties of the fly ash were expected to have a negative influence on agglomeration. Preliminary sizing with Andersen impactors of the test dusts was also performed by redispersing them in the laboratory with an air ejector similar to the one in the Braxton dust feed system. The results of these measurements (Appendix D) also indicated the suitability of the cupola dust.

Table 1. Sonic Agglomerator System Operating Parameters

RUN NO.	DATE	TEST DUST	VOLUME FLOW m^3/s	PRESSURE DROP ACROSS SONIC CHAMBER $n/m^2 \times 10^{-3}$	FAN POWER[a] KILOWATTS	STEAM		WATER		SONIC GENERATOR	
						PRESSURE $n/m^2 \times 10^{-3}$	FLOW $m^3/s \times 10^5$	PRESSURE $n/m^2 \times 10^{-4}$	FLOW $m^3/s \times 10^5$	INTENSITY db	POWER KILOWATTS
1	10/17/73	cupola	2.22	2.96	12.40		0		0	0	
2	10/17/73	cupola	2.22	2.96	12.40		0	10.34	8.20	164	3.25
3	10/18/73	cupola	2.22	2.96	12.40		0	10.34	8.20	164	2.90
4	10/24/73	cupola	2.22	2.96	12.40		0	10.34	8.20	166	2.90
5	11/2/73	cupola	2.23	1.09	4.94		0	10.34	4.42	165	3.60
6	11/13/73	cupola	2.23	1.09	4.94		0	10.34	4.42	0	
7	11/13/73	cupola	2.23	1.09	4.94		0	10.34	4.42	165	3.00
8	11/19/73	cupola	2.47	1.09	5.48	3.45	2.27	6.90	4.42	164	3.20
9	11/19/73	cupola	2.48	1.09	5.50	3.45	2.27	6.90	4.42	0	
10	11/29/73	cupola	2.48	1.09	5.50	48.26	11.35	6.90	4.42	164	3.10
11	1/2/74	cupola	DUST	FEEDER FAILURE							
12	1/2/74	cupola	0.82	0.12	0.20	3.45	2.27		0	c	3.20
13	1/4/74	cupola	3.72	2.53	19.19		0		0	0	
14	1/4/74	cupola	3.72	2.53	19.19	3.45	2.27	6.90	4.42	161	3.00
15[b]	1/22/74	fly ash	2.48	1.09	5.50		0		0	0	
16	1/22/74	fly ash	0.82	0.12	0.20	20.68	7.72		0	162	3.30
17[b]	2/19/74	cupola	2.47	1.09	5.48		0		0	0	
18	2/19/74	fly ash	2.47	1.09	5.48	3.45	2.27	10.34	4.42	164	3.20
19	2/19/74	fly ash	2.47	1.09	5.48	3.45	2.27	10.34	4.42	165	3.50

a Fan power based on motor-fan combined efficiency of fifty-five percent.

b Runs 15 and 17 were to determine mass efficiency by size of sampling cyclone only.

c Microphone broken - sound intensity unknown.

The high pressure drop across the sonic chamber during tests one through four was caused by an inlet manifold with a very small opening. Although this tortuous configuration may have increased the dust-spray interactions, the high shear forces encountered may actually break up any agglomerates entering the system. The inlet restriction also was an added burden on the fan capacity and was replaced by the normal inlet before test five.

The increase in volume flow starting with test eight reflects the installation and use of gas burners at the air intake. This was required to keep the temperature in the system high enough to prevent the condensation of the steam as soon as it was introduced. Runs 12 and 16 were at a low flow rate (2000 cfm) while 13 and 14 were at the highest flow rate the system could achieve (8000 cfm).

The fan power required at the indicated volume and static pressure was based upon an assumed motor-fan combined efficiency of 55 percent. The sound intensity and power demands of the sonic generator were taken from direct readings on the control panel of the Braxton device. The steam and water consumptions were determined by Braxton personnel with calibrated flow meters.

B. EFFECT OF THE SONIC AGGLOMERATOR ON PARTICULATE COLLECTION

Table 2 summarizes the inlet and outlet dust loading. The relatively large portion of the inlet dust that was captured by the cyclone indicates a fairly coarse particulate. While this was expected to be the case with fly ash it was unexpected for the cupola dust because laboratory dispersion tests with a relatively high ejector air pressure (90 psi) had shown a mass median diameter of just larger than one micrometer (Appendix D). The Braxton dust feed system was designed to have a similar air pressure to resuspend the dust, but the high pressure compressor was out of service during the early part of the tests. Therefore, the low pressure compressor at Braxton had to be utilized and the resulting air pressure (20 psi) to the air ejector probably failed to break up the agglomerates in the bulk dust and led to a coarser particulate than obtained in the laboratory. The high pressure

TABLE 2. COMPARISON OF INLET AND OUTLET DUST LOADING, CYCLONE CATCH, CYCLONE UNDERSIZE DUST AND OVERALL SYSTEM COLLECTION OF ALL PARTICLE SIZES.

RUN NO.	INLET			OUTLET			REDUCTION IN MASS OF FINE PARTICLES, PERCENT	REDUCTION OF TOTAL MASS, PERCENT	SYSTEM EFFICIENCY IF FOLLOWED BY CYCLONE, PERCENT
	A	B	C	D	E	F	$\frac{(A\ C)-(D\ F)}{A\ C} \times 100$	$\frac{A-D}{A} \times 100$	$\frac{A-(D-D\ E)}{A} \times 100$
	CONCENTRATION g/m^3	CYCLONE FRACTION	FILTER FRACTION	CONCENTRATION g/m^3	CYCLONE FRACTION	FILTER FRACTION			
1	1.3309	.836	.164	0.7707	.657	.343	-20.9	42.1	80.1
2	1.5859	.809	.191	0.1945	.368	.632	59.4	87.7	92.3
3	1.8343	.906	.094	0.2629	.756	.244	62.8	85.7	96.5
4	2.2744	.869	.131	0.3121	.568	.432	54.9	86.3	94.1
5	1.1202	.887	.113	0.2124	.626	.374	37.0	81.0	92.9
6	1.1982	.794	.206	0.3806	.569	.431	33.6	68.2	86.3
7	1.6875	.850	.150	0.4639	.713	.287	47.2	72.5	92.1
8	1.2012	.902	.098	0.1648	.391	.609	14.6	86.3	91.6
9	0.8792	.875	.125	0.1499	.472	.528	28.1	83.0	91.0
10	1.5213	.886	.114	0.2352	.507	.493	33.0	84.5	92.4
12	0.9227	.698	.302	0.5824	.702	.298	37.8	36.9	81.2
13	2.5218	.931	.069	1.0376	.756	.244	-45.8	58.9	90.0
14	2.0105	.942	.058	0.1856	.723	.277	55.3	90.8	97.4
16	2.5690	.983	.017	0.2799	.899	.101	34.0	89.1	98.9
18	6.0677	.951	.049	0.3936	.879	.121	84.0	93.5	99.2
19	5.4163	.965	.035	0.4069	.922	.078	83.2	92.5	99.4

compressor became available later in the program but it was decided that a change in operating parameters part way through the tests would be unwise so the low pressure air supply was utilized throughout.

In addition to the mass concentration, the cyclone fraction and the filter fraction at the inlet and outlet, Table 2, shows the percent reduction of total mass and the percent reduction of fine particles. The reduction of total mass is that portion of the dust that was removed in the sonic chamber by wash out, settling, precipitation, impaction or whatever other mechanisms may be involved. It is a measure of the AVP as a dust collector rather than a conditioner. An average of 86 percent of the cupola dust and 97 percent of the fly ash is cyclone collectable before treatment by the AVP so it is important to examine the reduction in mass of fine particles. This is merely the percent reduction of the cyclone undersize dust at the outlet of the AVP as compared to that of the cyclone undersize dust at the inlet.

Also computed in Table 2 is the system collection efficiency if it were followed by a cyclone displaying the same collection efficiency as the cyclones in the sampling trains. This takes into account both the dust lost in the sound chamber and the increased collectability of the effluent as a result of the reduction of small particles. It is important to keep in mind when using the efficiencies shown that the inlet cyclone fraction shown in column B would be the system efficiencies without any conditioning whatsoever.

Two tests (1 and 13) were run in which no sound, steam or water were used to determine what effect the physical configuration of the Braxton system has on the test aerosol. It is interesting to note that under those conditions the system retains about half of the total dust entering it but the dust that penetrates the chamber has a substantially higher portion of its mass in the cyclone undersize range. This shows up as a negative number in the reduction in mass of fine particles. This would indicate that the physical configuration works against agglomeration by breaking up aggregates that enter.

Test six was run with water spray but no sound or steam. This shows the positive contribution of the sprays both in increasing the percent of the

dust retained in the chamber and also in decreasing the fraction of fine material. The positive influence of the water sprays can also be seen by examining tests two, three and four. The average reduction in the percent of cyclone undersize dust is considerably greater (59 percent versus 37 percent) than those tests run with the same test dust with sound but with half the water spray volume (tests 5, 7, 8, 10 and 14). Figure 2 shows the percent reduction in the mass of fine particles as a function of water flow rate disregarding other system parameters. Although the data show considerable scatter, there is a trend toward more efficient reduction of fines at increased water flow rates. The correlation coefficient of the 13 pairs that showed a positive reduction in fine particles is 0.43, while the correlation coefficient of the data for all tests, including negative reduction in fines, is 0.65. The former correlation coefficient is not statistically significant while the latter is statistically significant ($\alpha = .05$).

Test nine was run with steam and water but no sound to compare the results with test six without steam or sound. The steam appears to substantially increase the percent mass retained in the chamber but has a slight negative influence on the reduction of fine particles. Figure 3 shows the percent reduction in the mass of fine particles as a function of steam flow rate disregarding other system parameters. Disregarding the two tests that resulted in negative fine particle reduction, the correlation coefficient is - 0.30. The correlation coefficient of the data for all runs, including those with negative reduction in fines, is 0.06. Neither coefficient is statistically significant.

Tests 16, 18 and 19 were run with fly ash and the larger particle size distribution of this test dust is obvious. Test 19 was a repeat of test 18 because of difficulties experienced during test 18. The data are included for completeness but are in doubt because the outlet sampling train nozzle was misaligned during part of the test run. The strong influence of the water sprays can also be seen by comparing the reduction of fine particles in run 16 (34 percent) without water but with steam and sound versus run 19 (83 percent) with water, steam and sound. This is in spite of the fact that run 16 was at a low flow rate so the residence time in the chamber was about two and one half times as long as for run 19.

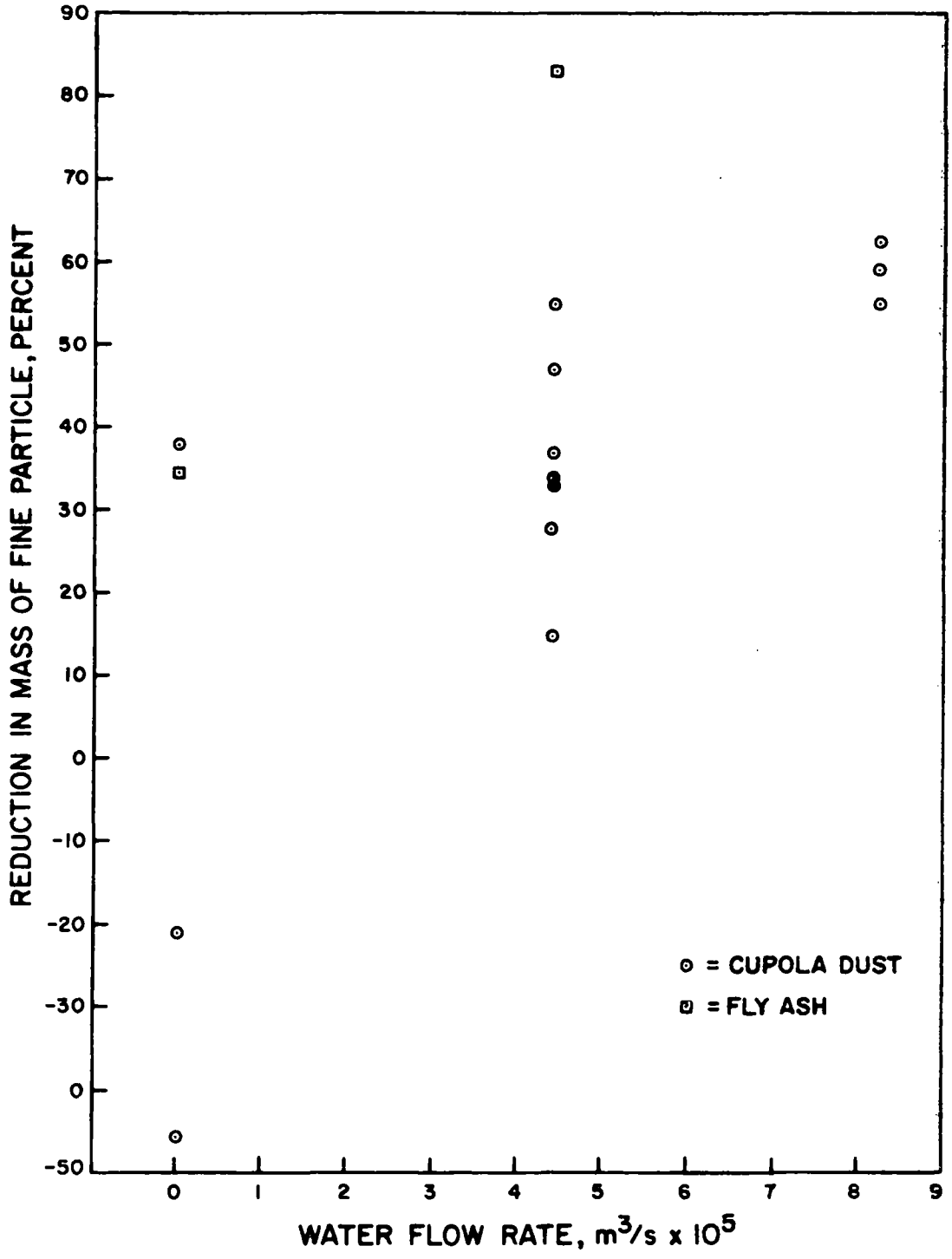

Figure 2. Effect of Water Flow Rate on the Reduction of Fine Particles.

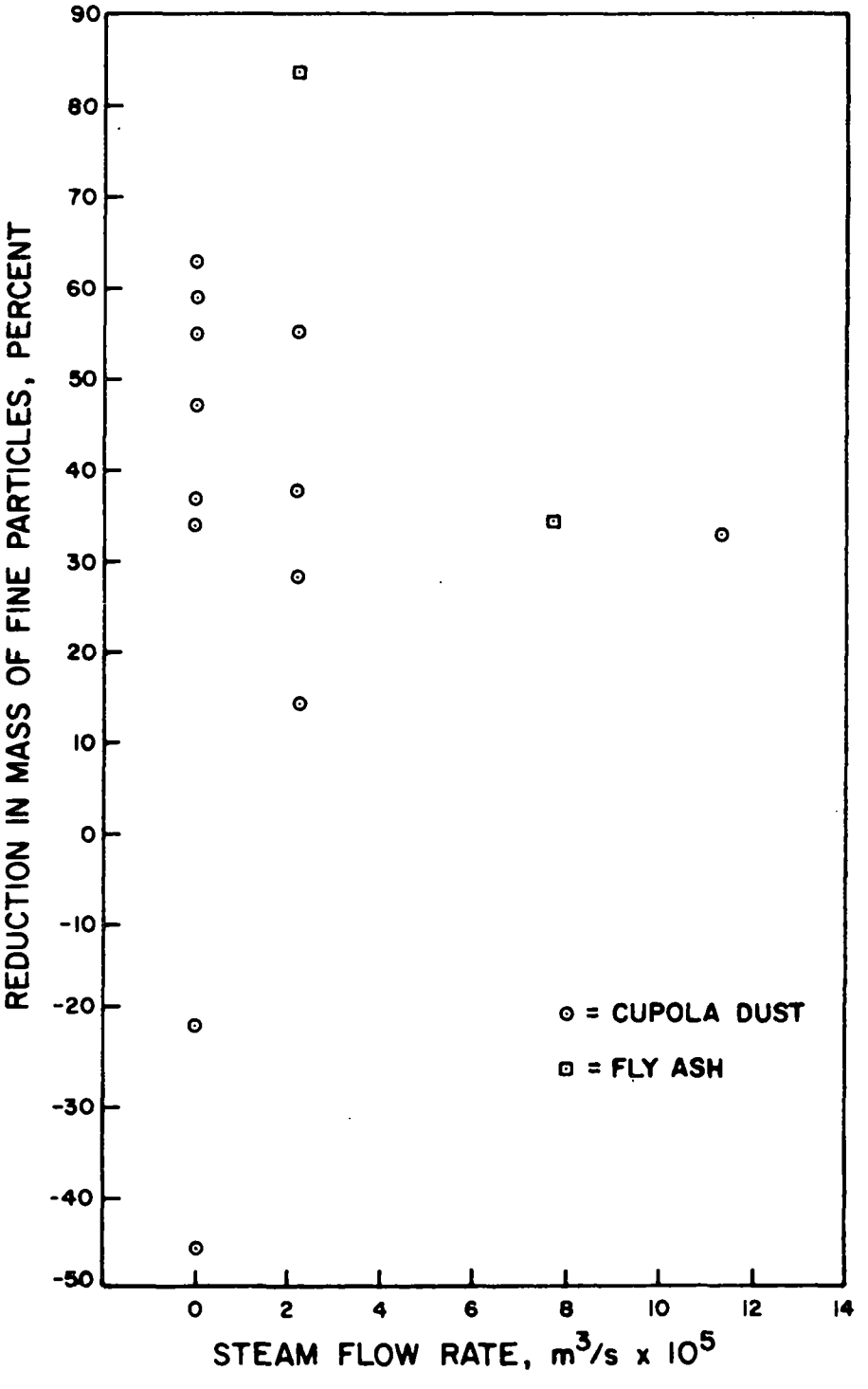

Figure 3. Effect of Steam Flow Rate on the Reduction of Fine Particles.

The influence of the sonic generator can be seen by comparing test 6 (water, no sound, no steam) with tests 5 and 7 (water, sound, no steam). The addition of sound increased the reduction of fine particles and increased the amount of dust retained in the chamber. The use of sound, however, did not appear to play as significant a role in the depletion of small particles as the addition of water. Test 6, in which water was added but no steam and no sound was used, showed a 33.6 percent reduction in fines. The use of sound and water in tests 5 and 7 averaged 42.3 percent reduction in fines. Tests 2, 3 and 4 were run with sound and twice the water rate as tests 5 and 7 and showed a 59.2 percent reduction in fines. Figure 4 shows the percent reduction in the mass of fine particles as a function of the sonic generator power consumption disregarding other system parameters. For the 13 tests that showed a positive influence on the fines reduction the correlation coefficient is 0.33, while the correlation coefficient of the data for all tests is 0.68. The former coefficient is not statistically significant and the latter is statistically significant.

Since most of the tests were run with cupola dust, a more detailed statistical analysis was undertaken for those 13 tests. A multiple regression analysis was used on the data of the cupola dust tests and showed the following relationship:

$$\%\ \text{reduction in mass of fine particles} = -15.1 + 6.5\left(\text{water flow, } m^3/s \times 10^5\right) + 8.3\ \text{(sonic generator power, kilowatts)}$$

An analysis of variance shows that the regression is highly significant (99 percent). It should be noted that the first member on the right side of the equation is negative and thus shows the detrimental influence on fine particle reduction of the physical configuration of the unit as was demonstrated when tests were run with no sound, water or steam. Furthermore, steam consumption does not appear in the relationship because it does not contribute significantly to the regression. The model also shows that the use of the sonic generator has somewhat less influence on fine particle reduction than does the use of water sprays, although the interaction of both plays a significant role

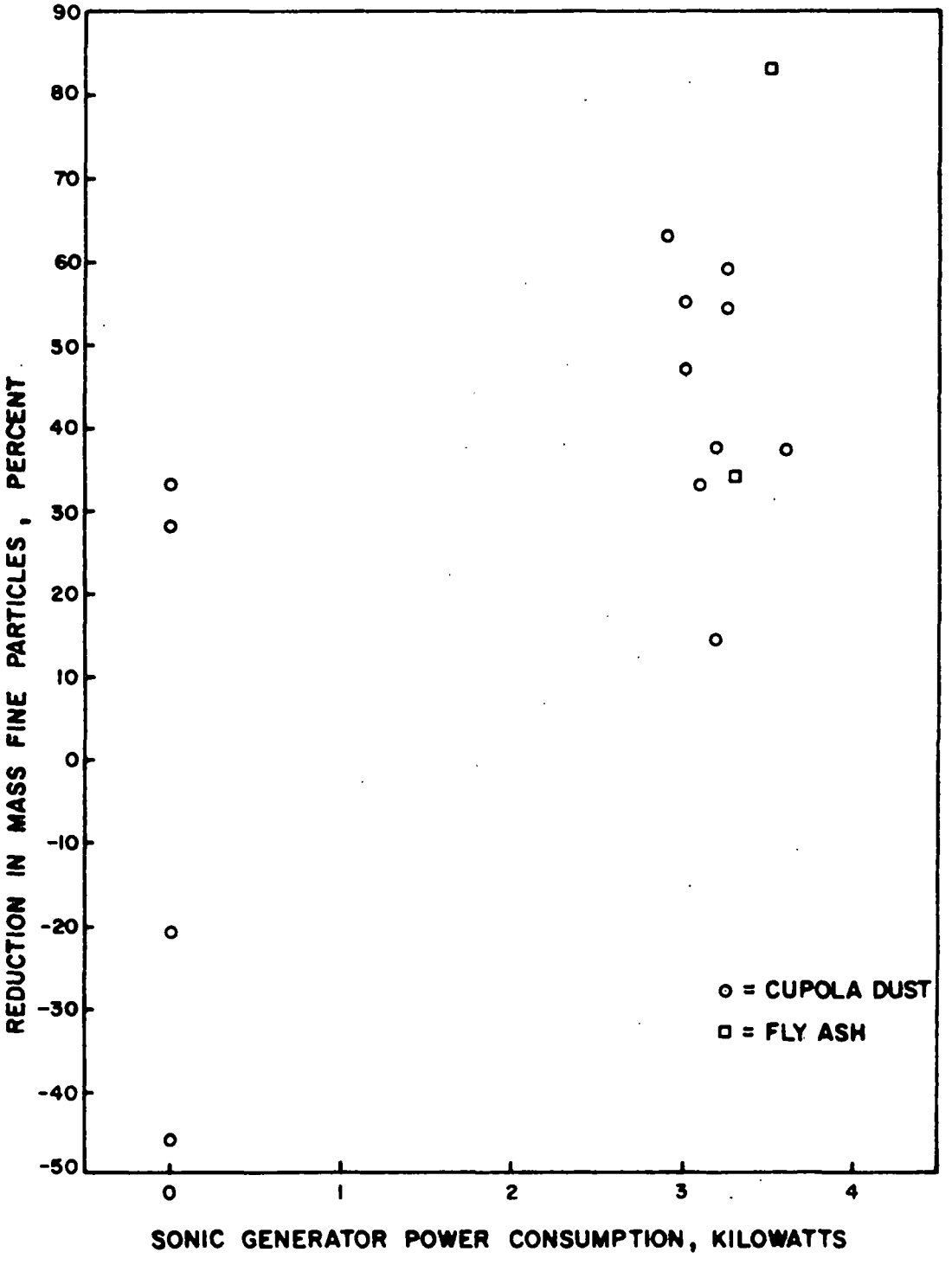

Figure 4. Effect of Sonic Generator Power Consumption on Reduction of Fine Particles.

Increasing the volume flow rate from 2.2 m^3/s (5,000 cfm) to 3.7 m^3/s (8,000 cfm) and hence decreasing the residence time in the chamber did not seem to adversely affect the performance of the AVP system when run with steam, water and sound. Run 14 was at the elevated flow rate with steam, water and sound and the reduction in the mass of fine particles was 55.3 percent. However, the elevated flow rate in test 13 when the system was run dry (no water, no steam, no sound) increased the mass of fine particles by 45 percent which indicates the breakup of agglomerates that enter the chamber.

Two tests were run at 0.82 m^3/s (2,000 cfm) and again the effect of residence time is obscure. Tests 12 and 16 were run at the reduced flow with steam and sound and the average reduction of fines was 35.9 percent. This indicates that the increased residence time with sound and steam is about as effective in reducing the fine particles as running with water only at a residence time of two and one half times less (test 6). In fact, running the system at a high flow rate with sound, steam and water (test 14) produced considerably better results than running at a low flow rate with sound and steam (tests 12 and 16).

C. EFFECT OF THE SONIC AGGLOMERATOR ON THE SIZE OF SMALL PARTICLES

In addition to examining the change in the mass of the small particles, it is of interest to investigate what changes, if any, are made in the size distribution of the cyclone undersize material. Effective agglomeration would be expected not only to decrease the mass of the small particles that penetrate the cyclone but also to increase the particle size of that portion that remains cyclone undersize at the outlet of the AVP.

Six stage Andersen cascade impactors were used downstream of the cyclone in both the inlet and outlet sampling trains, except for tests one and three when only outlet impactor samples were taken. Table 3 compares the concentration of cyclone undersize dust as measured with the glass fiber high volume filter and with Andersen impactors. The particle size distributions determined by the impactors are shown graphically in Figures 5 through 21 and in tabular form in Appendix C. Figures 18 and 20, corresponding to tests 15 and 17, show the particle size distribution upstream and downstream of the sampling

Table 3. COMPARATIVE CONCENTRATION MEASUREMENTS OF CYCLONE UNDERSIZE DUST WITH GLASS FIBER FILTERS AND ANDERSEN IMPACTORS

RUN NO.	INLET		OUTLET	
	FILTER, g/m^3	CASCADE IMPACTOR, g/m^3	FILTER, g/m^3	CASCADE IMPACTOR, g/m^3
1[b]	0.22	-	0.26	0.79
2[a,b]	0.30	0.23	0.12	0.29
3[b]	0.17	-	0.06	0.06
4[a]	0.30	0.24	0.14	0.06
5[b]	0.13	0.11	0.08	0.05
6	0.25	0.20	0.16	0.13
7	0.25	0.17	0.13	0.11
8	0.12	0.04	0.10	0.07
9	0.11	0.06	0.08	0.05
10	0.17	0.14	0.12	0.06
12	0.28	0.20	0.17	0.14
13	0.17	0.16	0.25	0.22
14	0.12	0.05	0.05	0.04
16	0.04	0.04	0.03	0.02
18	0.30	0.18	0.05	0.03

[a]denotes different sampling periods for impactor and filter at inlet

[b]denotes different sampling periods for impactor and filter at outlet

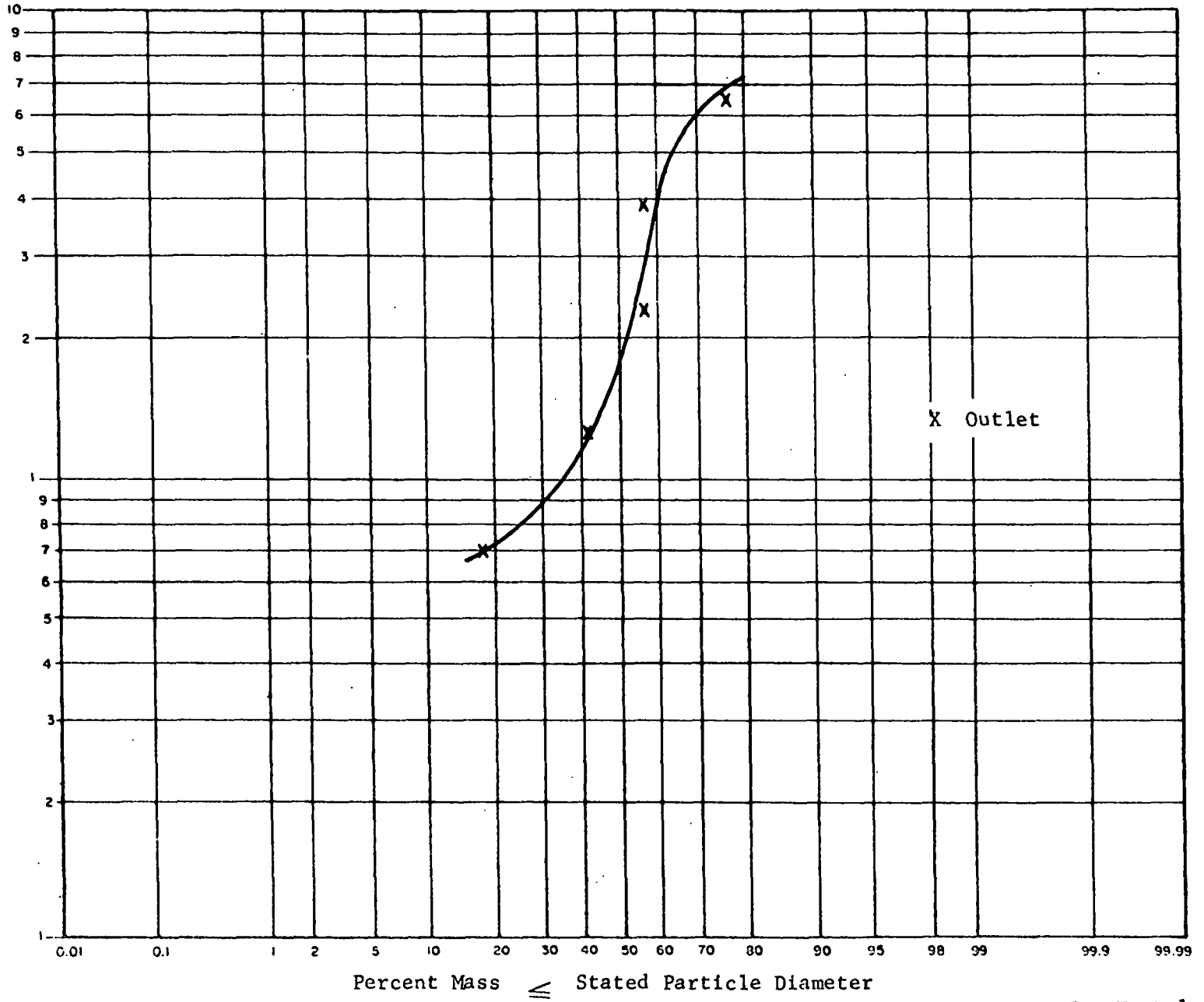

Figure 5. Particle Size Distribution of Cyclone Undersize Dust for Test 1

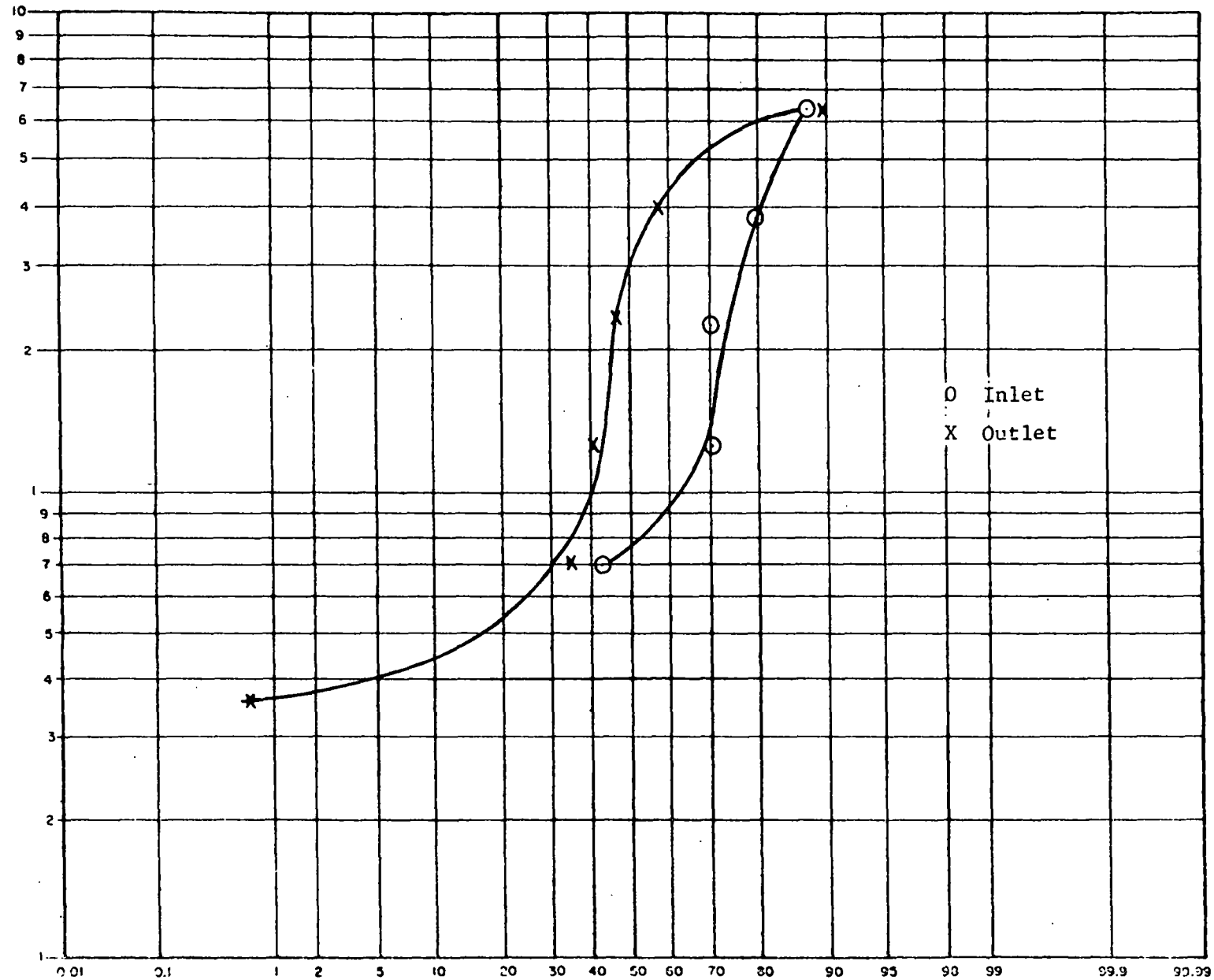

Figure 6. Particle Size Distribution(s) of Cyclone Undersize Dust for Test 2

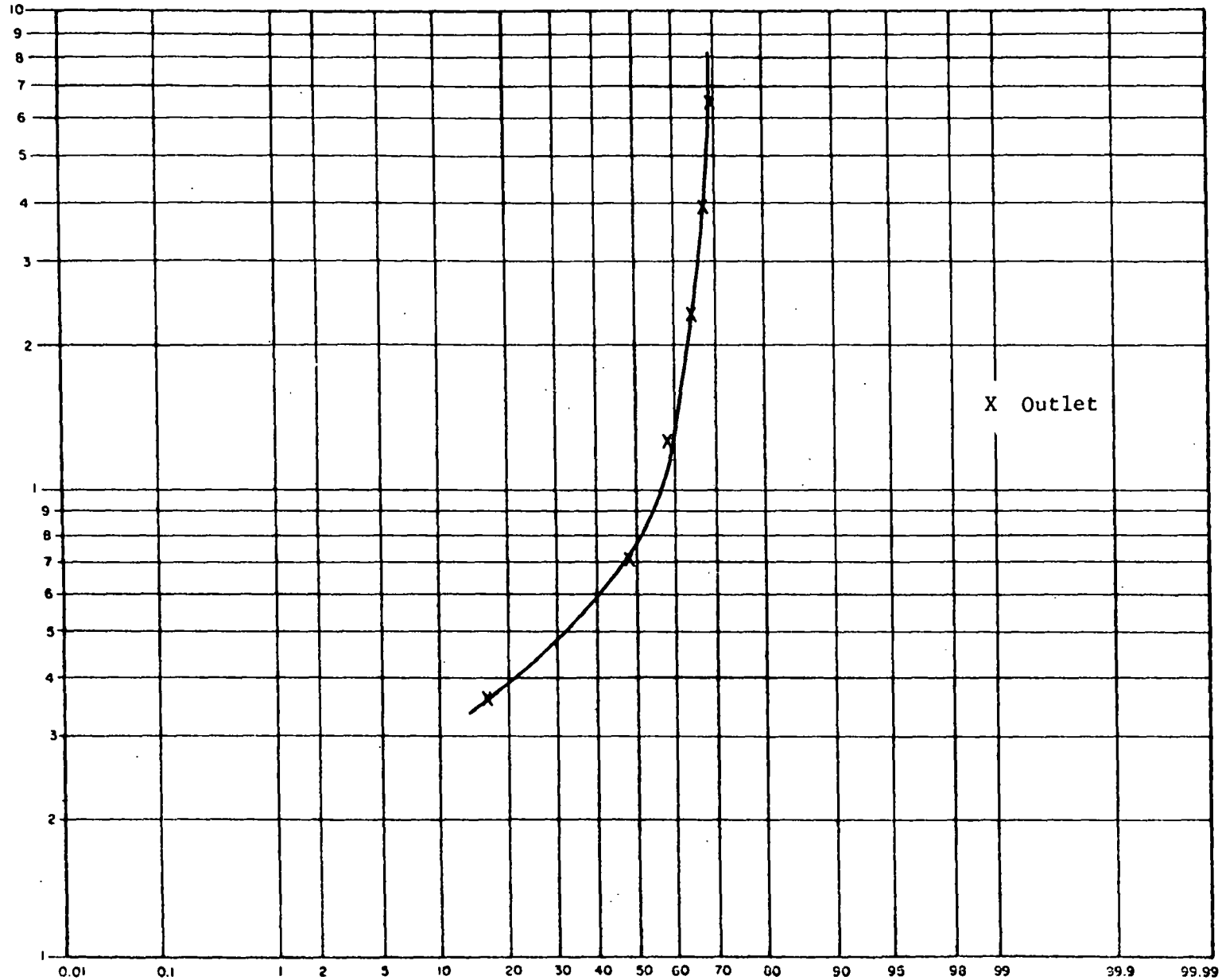

Figure 7. Particle Size Distribution(s) of Cyclone Undersize Dust for Test 3

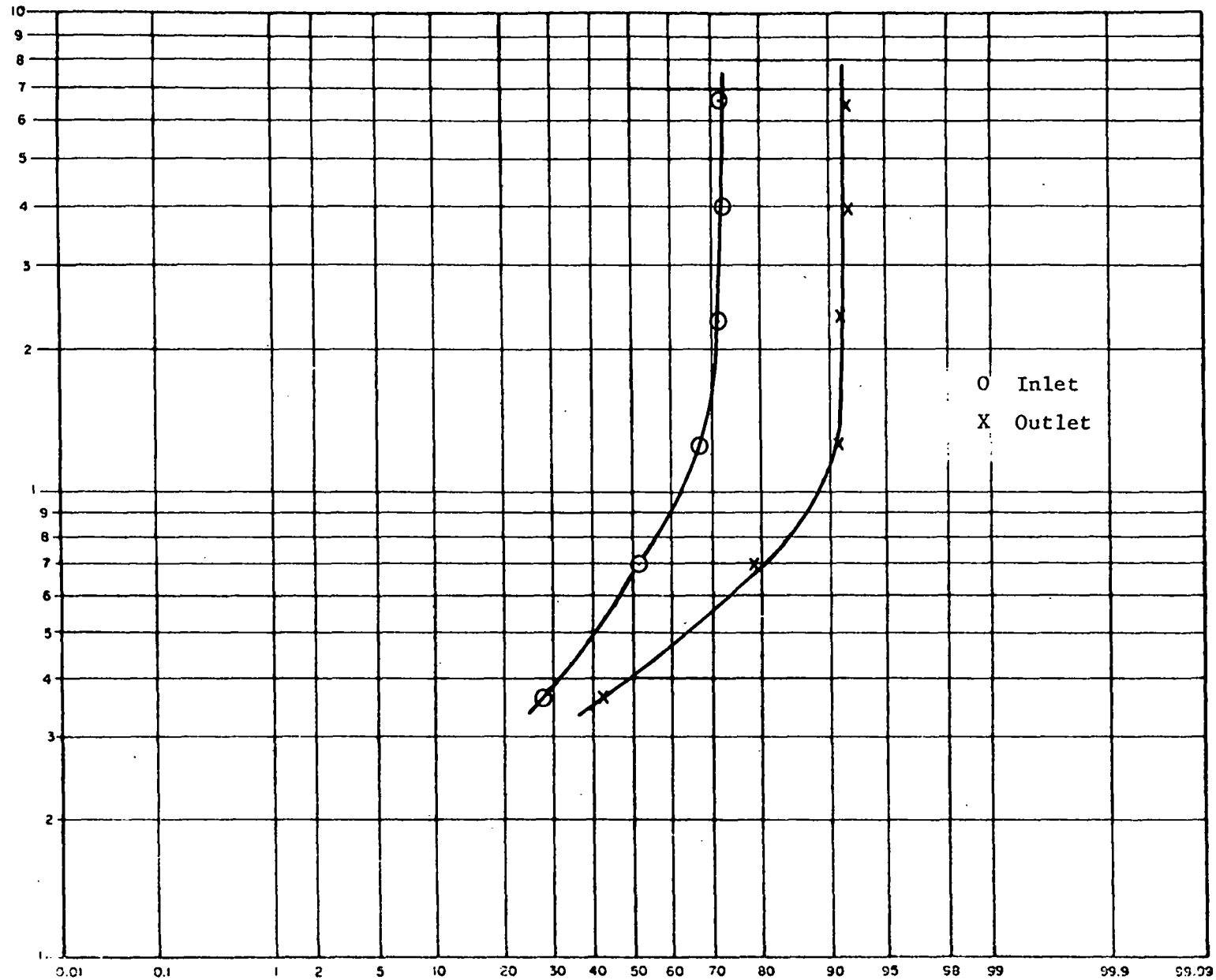

Figure 8. Particle Size Distribution(s) of Cyclone Undersize Dust for Test 4

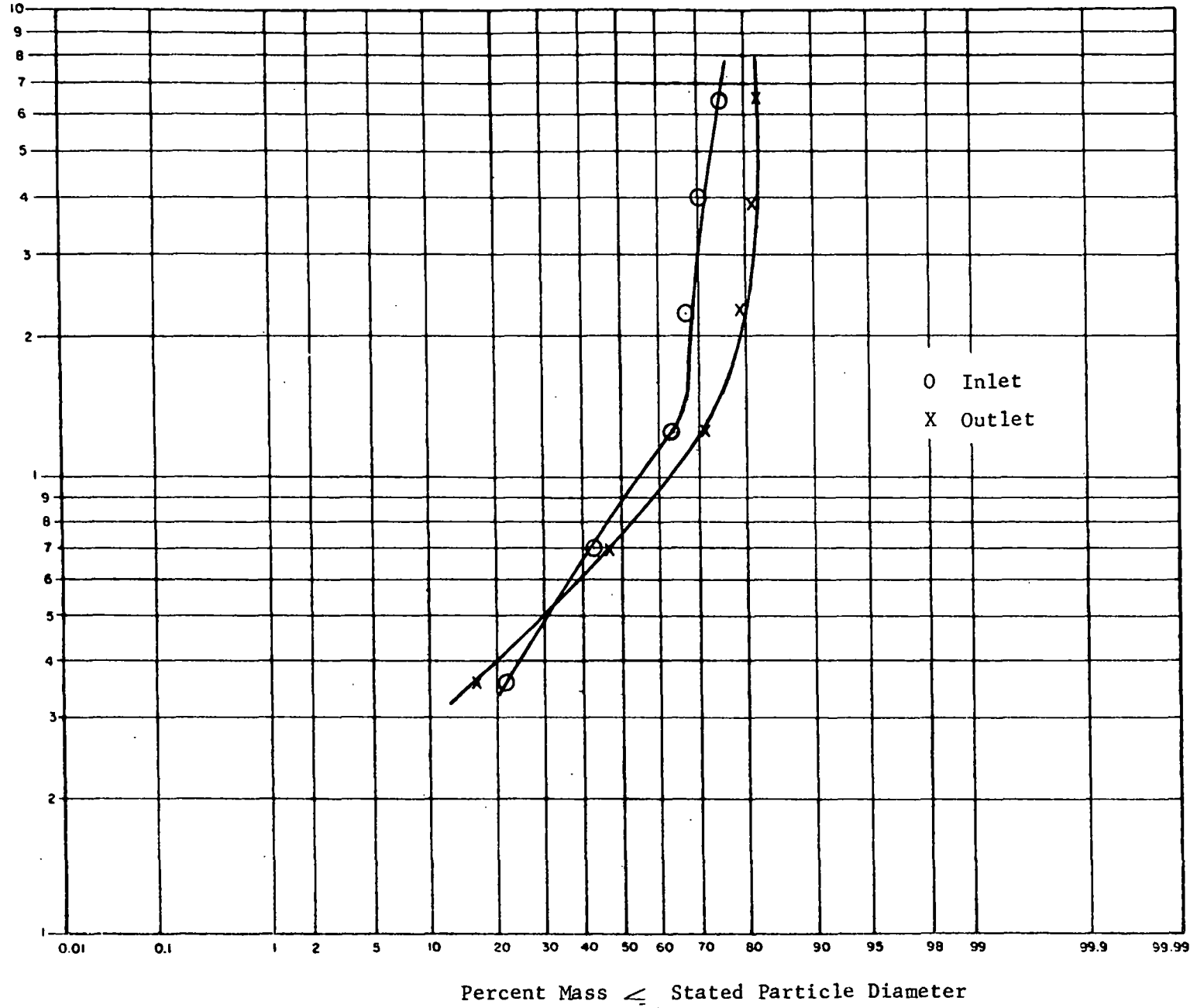

Figure 9. Particle Size Distribution(s) of Cyclone Undersize Dust for Test 5

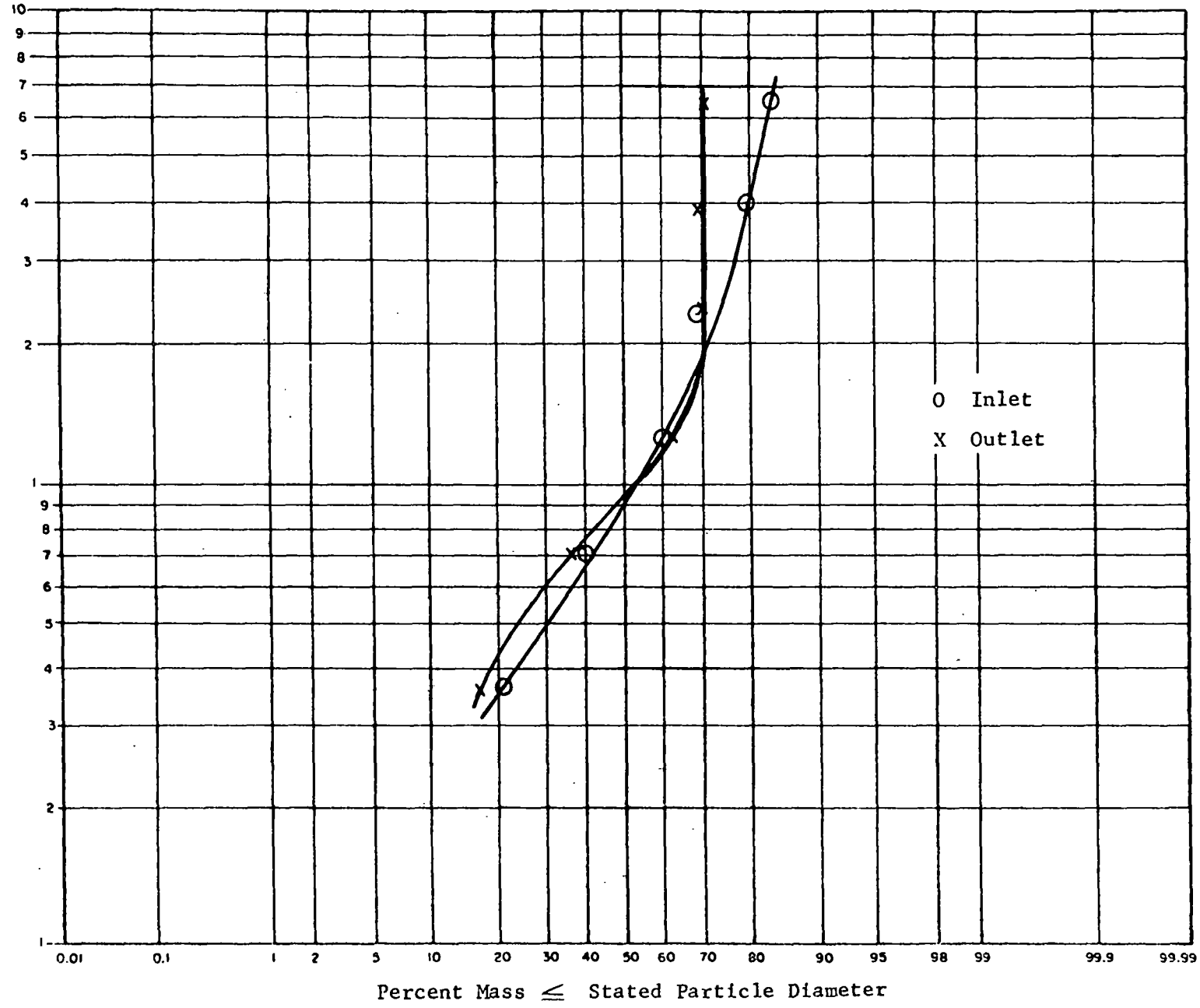

Figure 10. Particle Size Distribution(s) of Cyclone Undersize Dust for Test 6

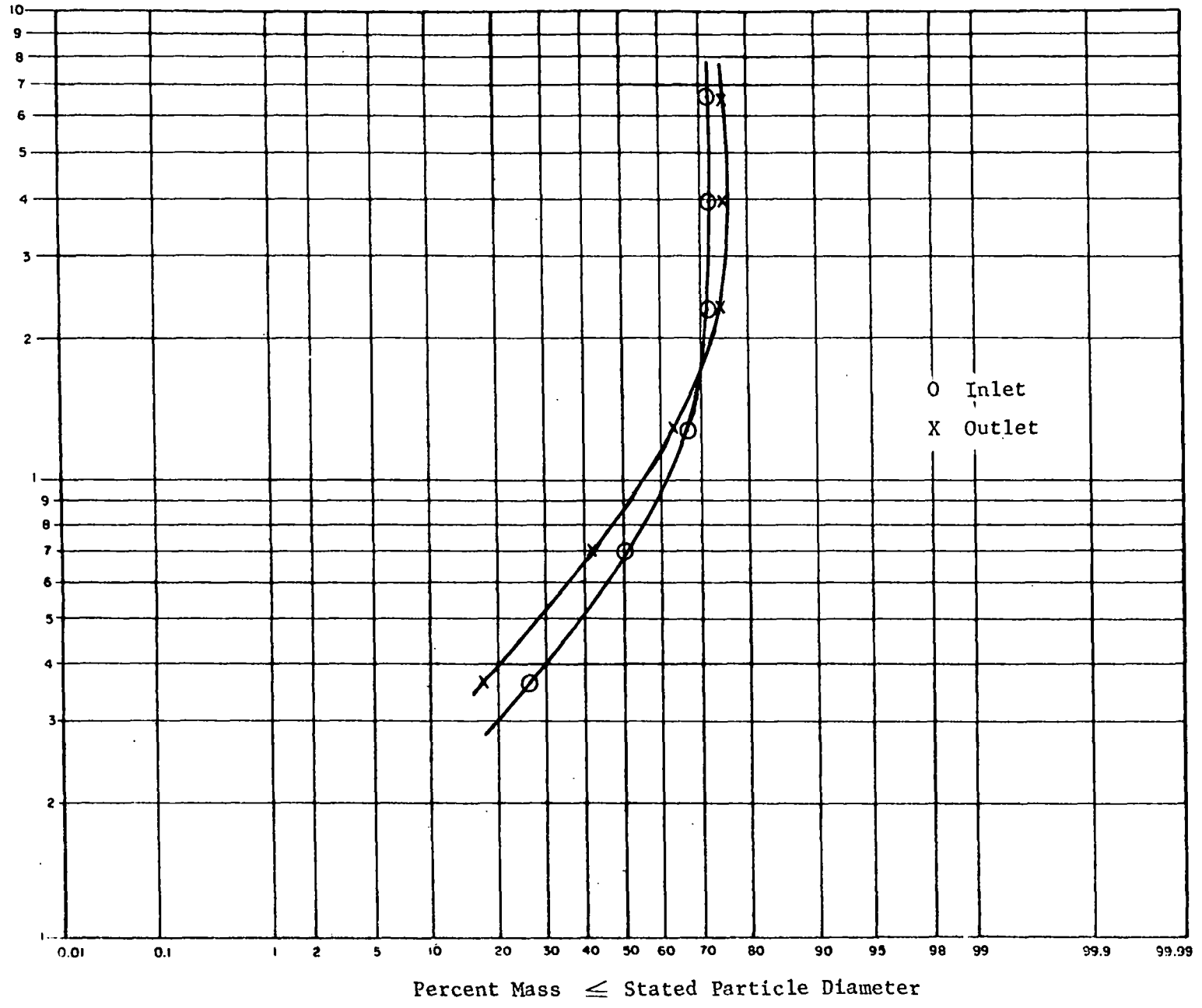

Figure 11. Particle Size Distribution(s) of Cyclone Undersize Dust for Test 7

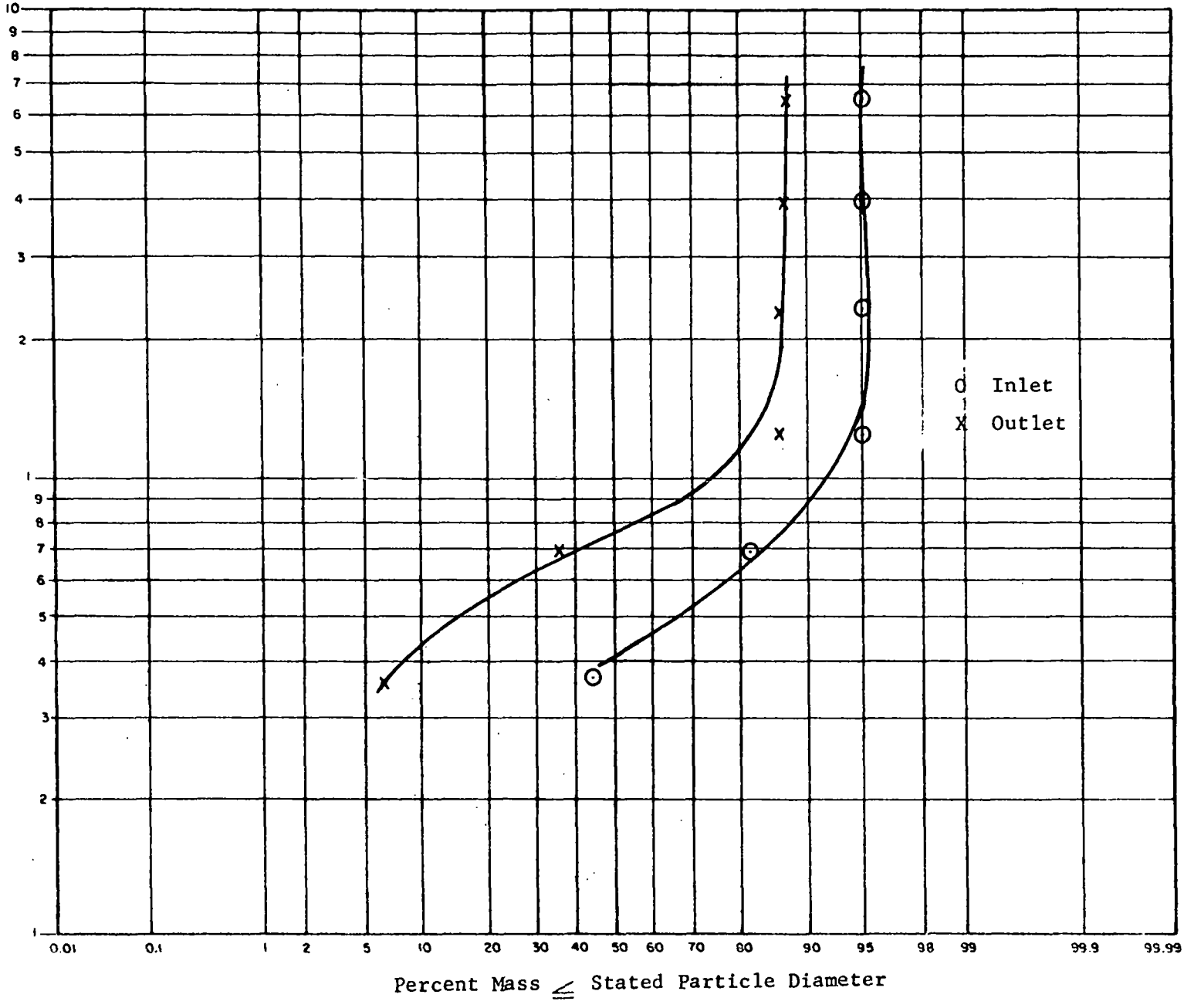

Figure 12. Particle Size Distribution(s) of Cyclone Undersize Dust for Test 8

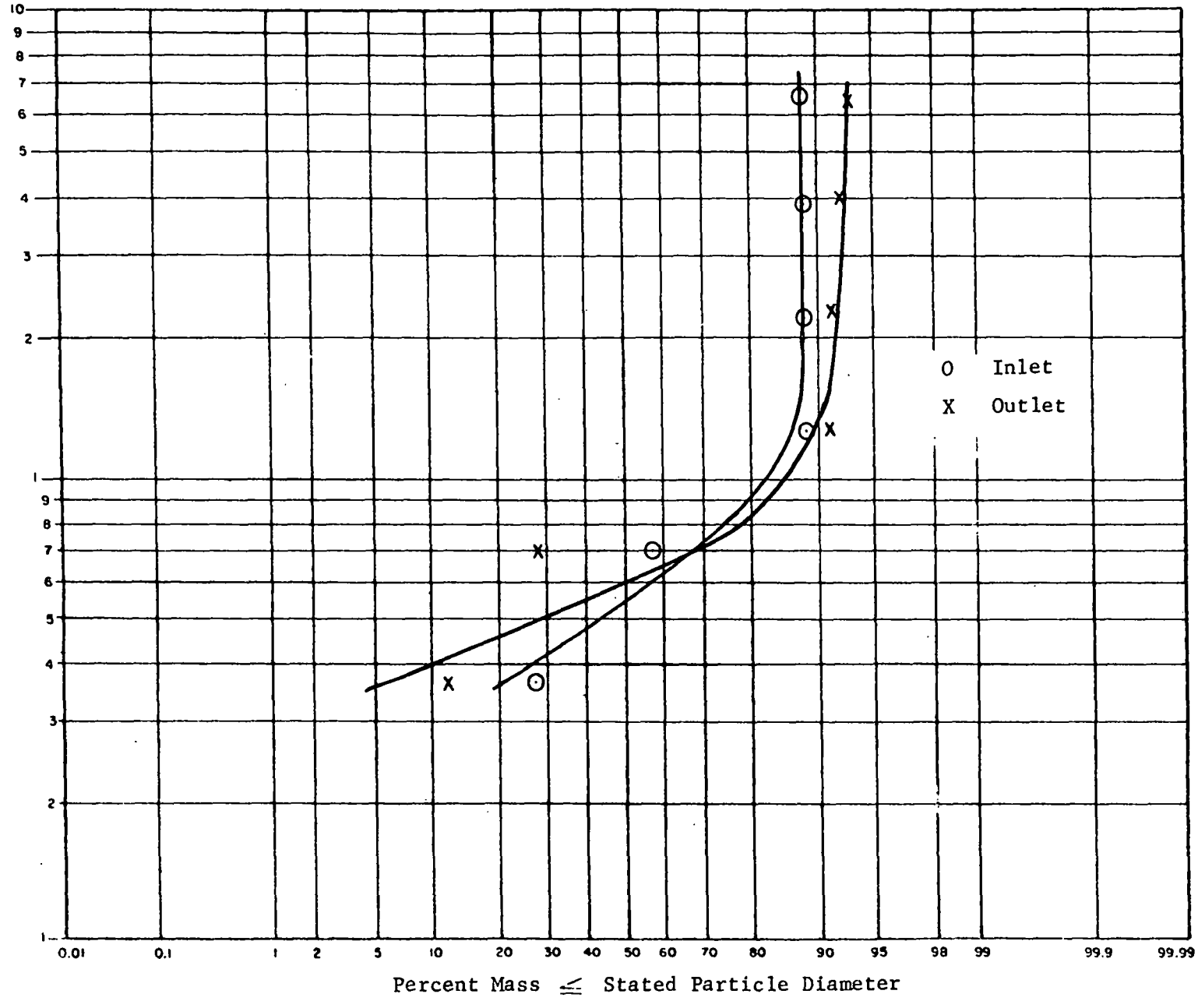

Figure 13. Particle Size Distribution(s) of Cyclone Undersize Dust for Test 9

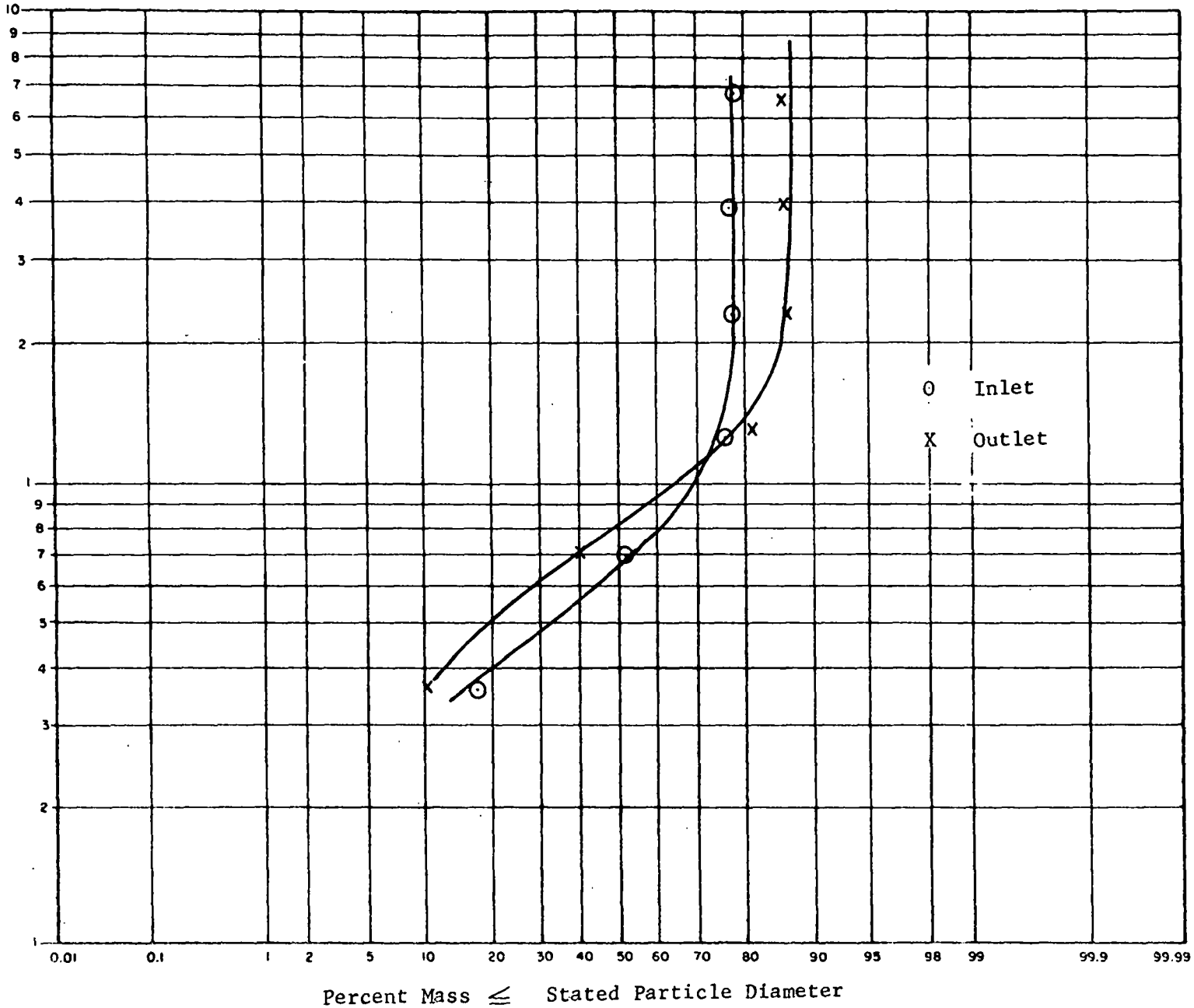

Figure 14. Particle Size Distribution(s) of Cyclone Undersize Dust for Test 10

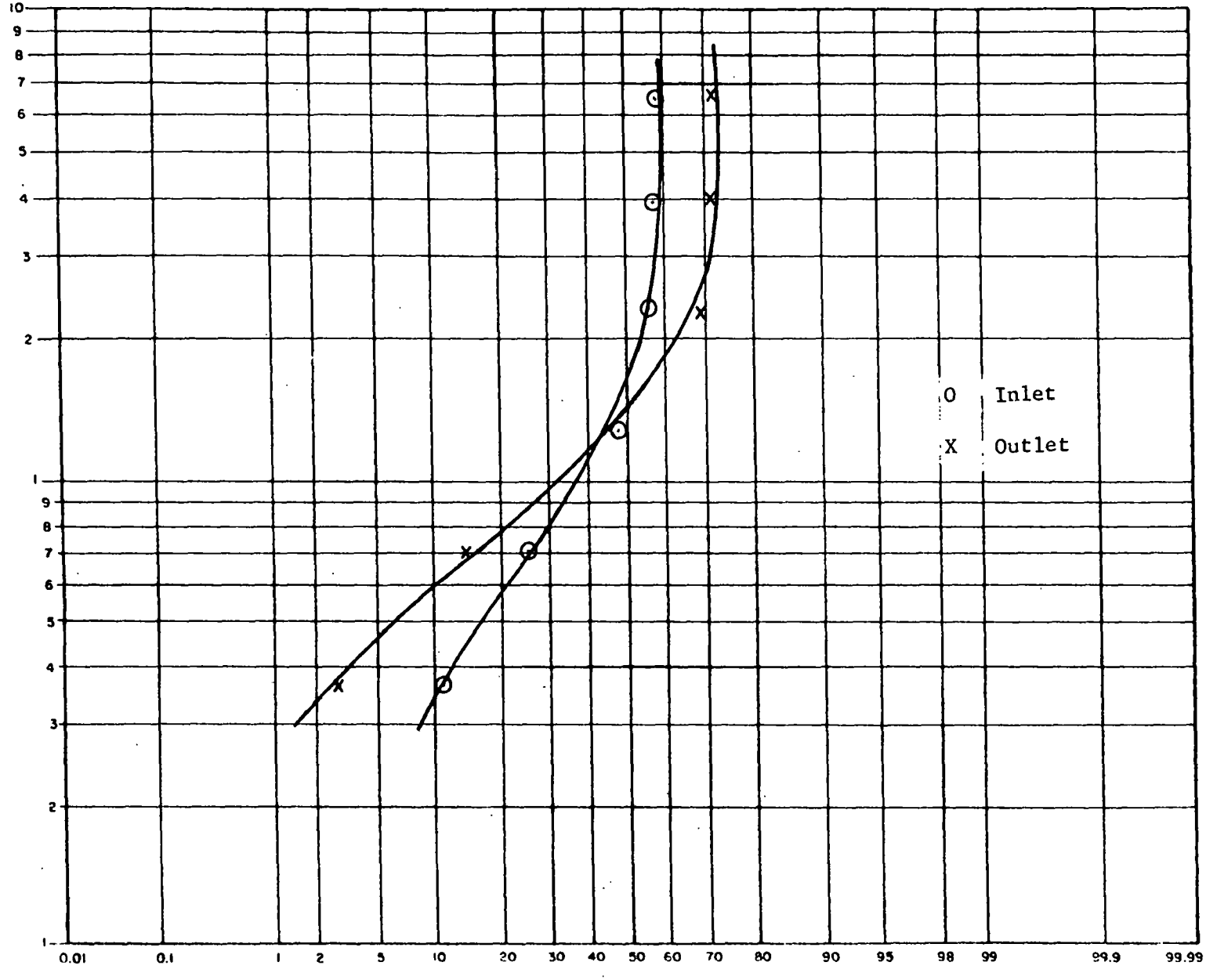

Figure 15. Particle Size Distribution(s) of Cyclone Undersize Dust for Test 12

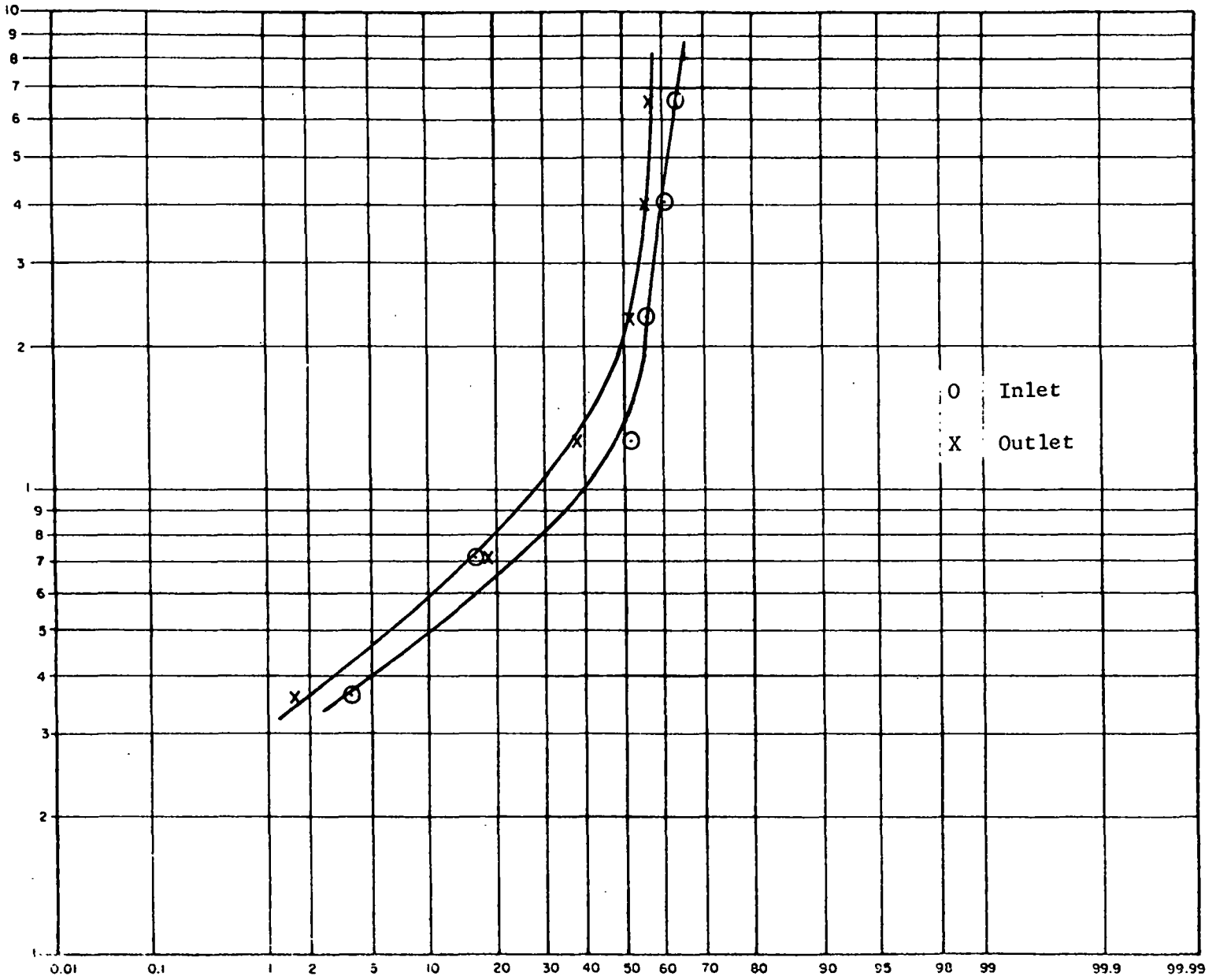

Figure 16. Particle Size Distribution(s) of Cyclone Undersize Dust for Test 13

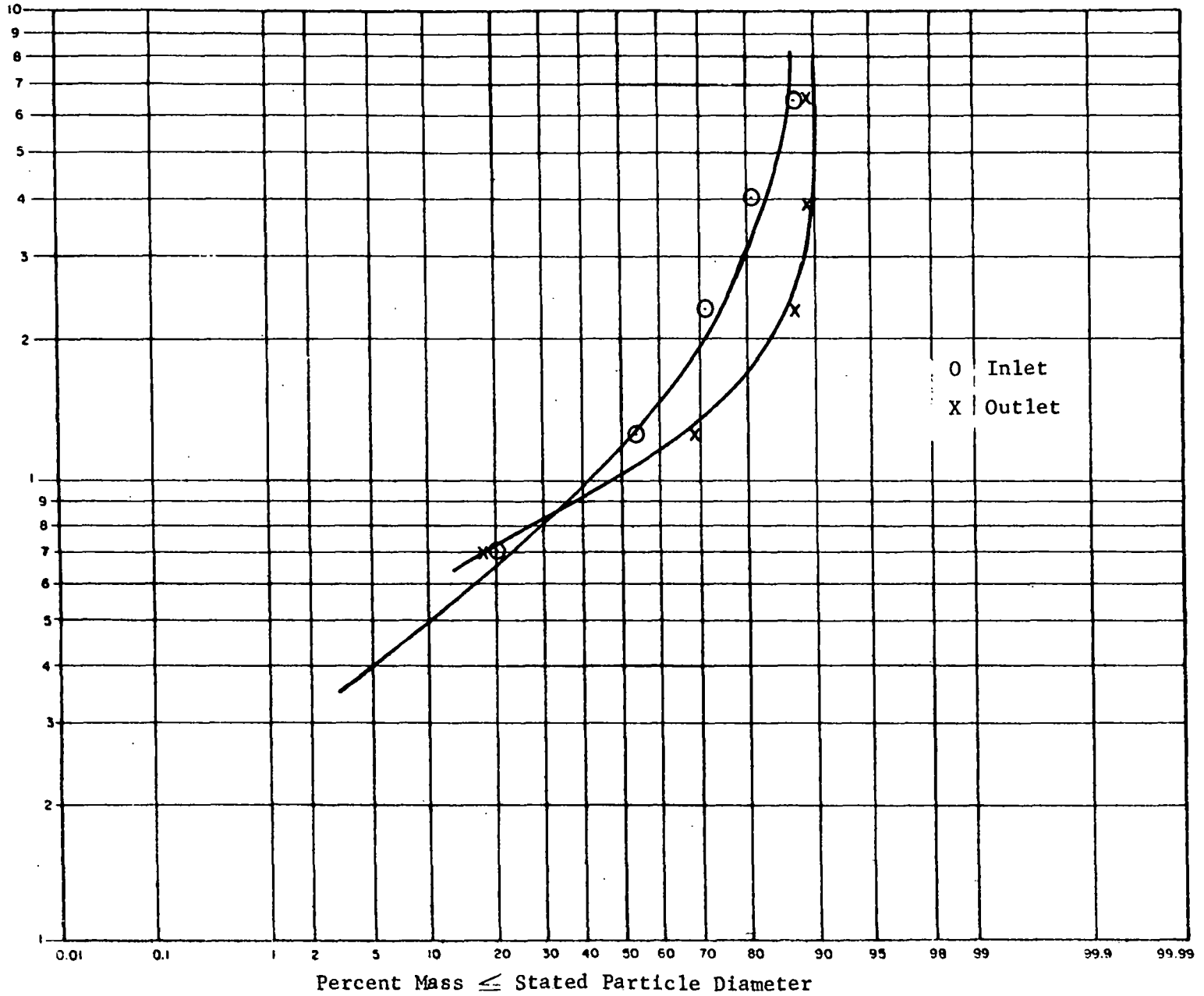

Figure 17. Particle Size Distribution(s) of Cyclone Undersize Dust for Test 14

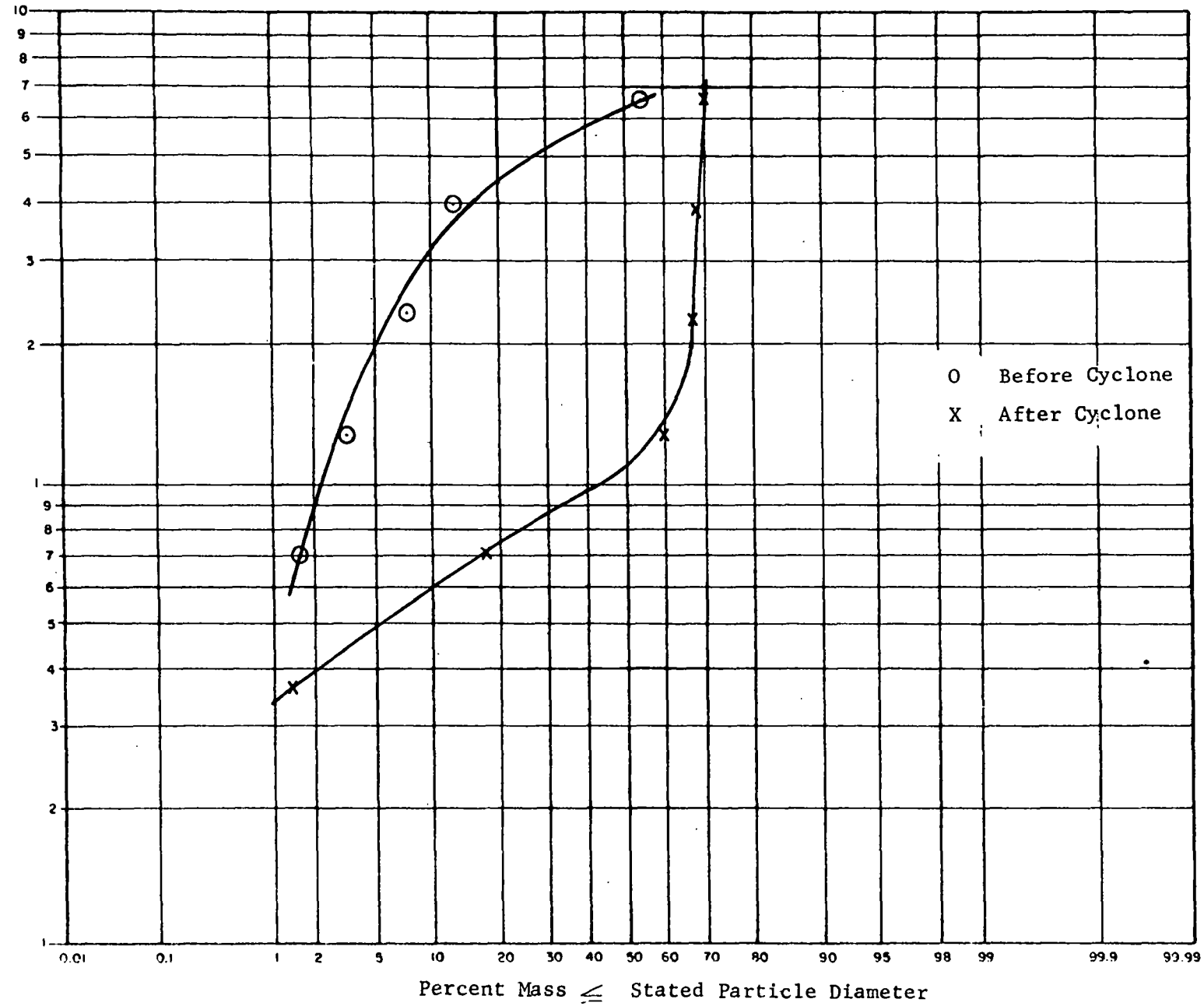

Figure 18. Particle Size Distribution(s) of Cyclone Undersize Dust for Test 15

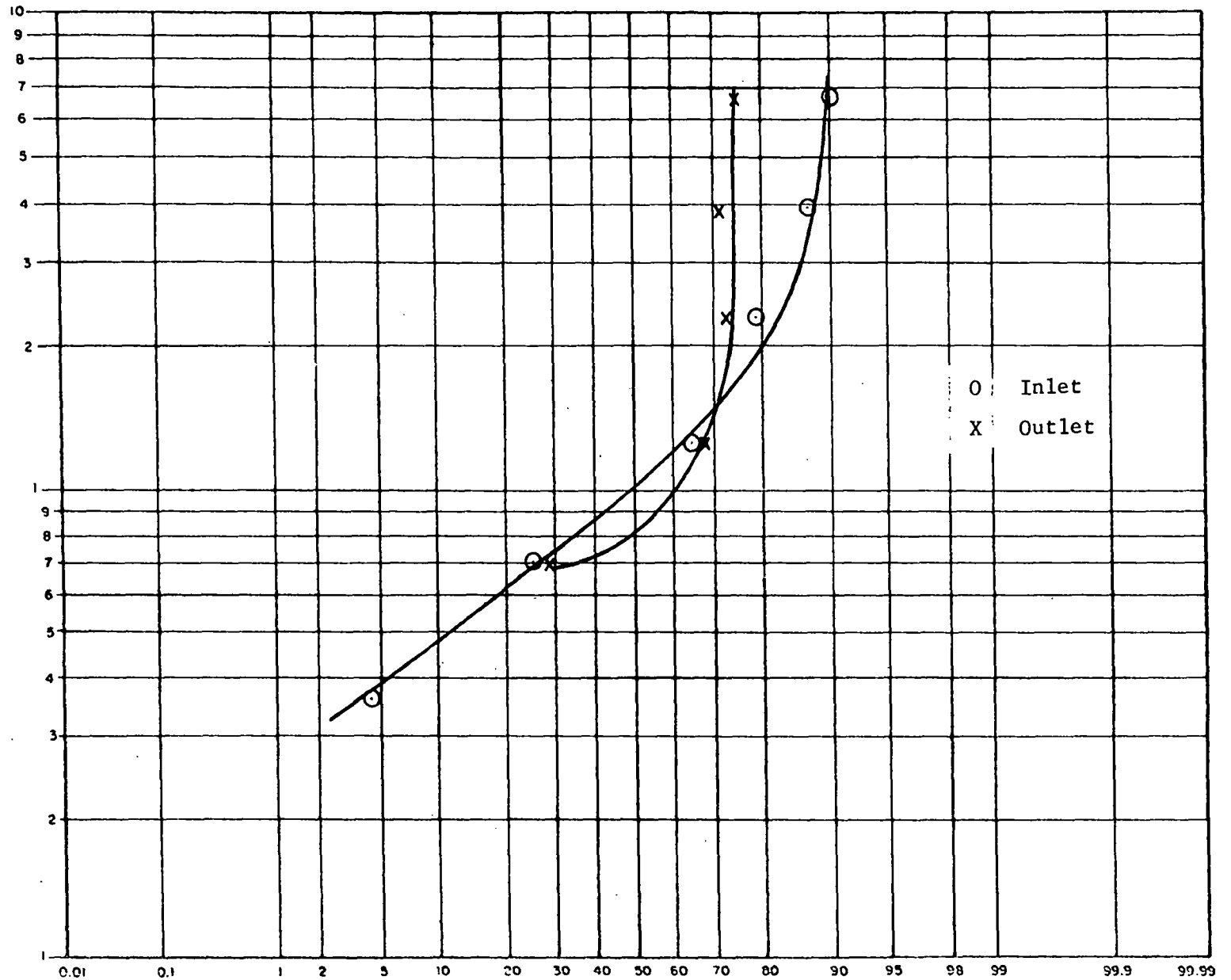

Figure 19. Particle Size Distribution(s) of Cyclone Undersize Dust for Test 16

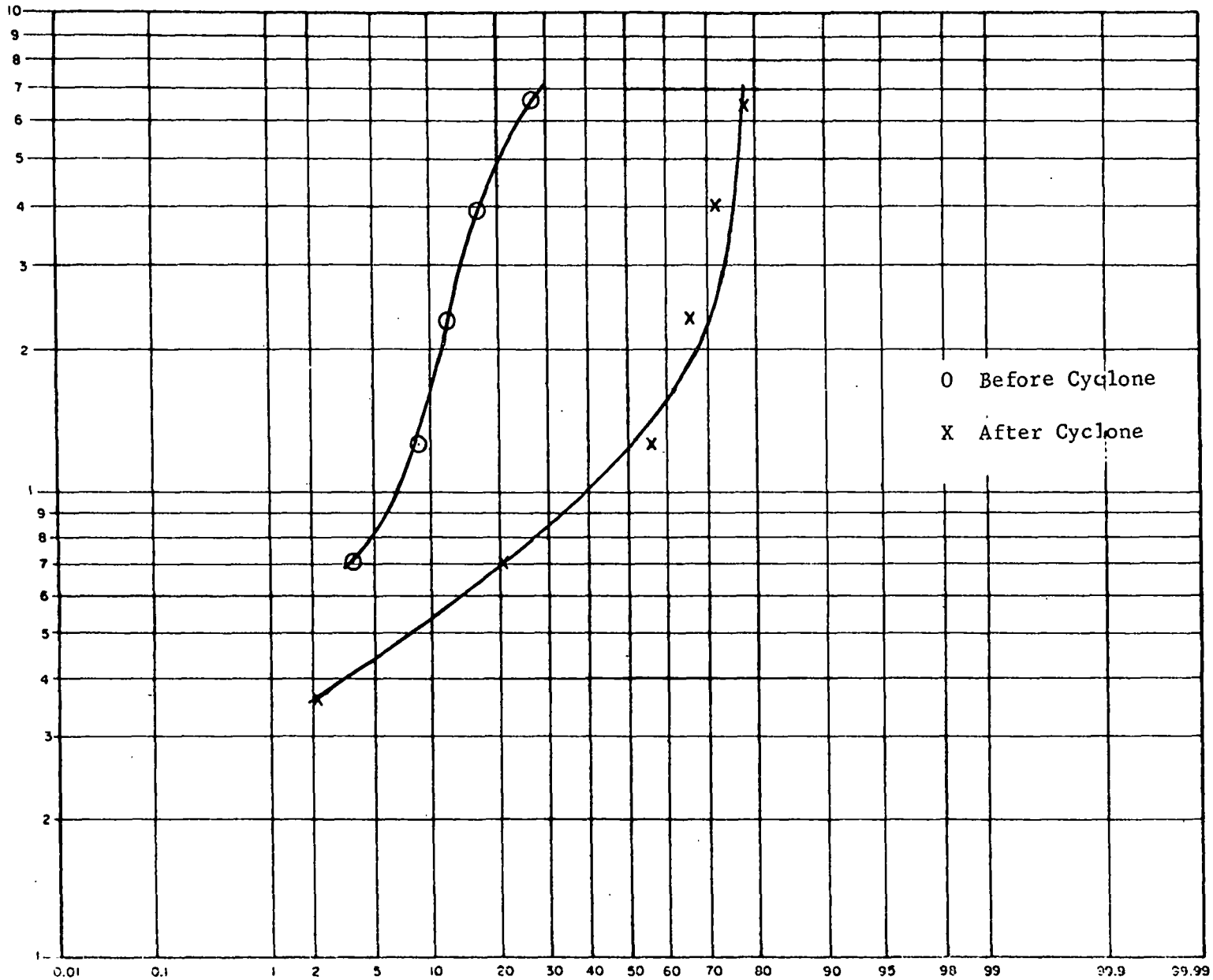

Figure 20. Particle Size Distribution(s) of Cyclone Undersize Dust for Test 17

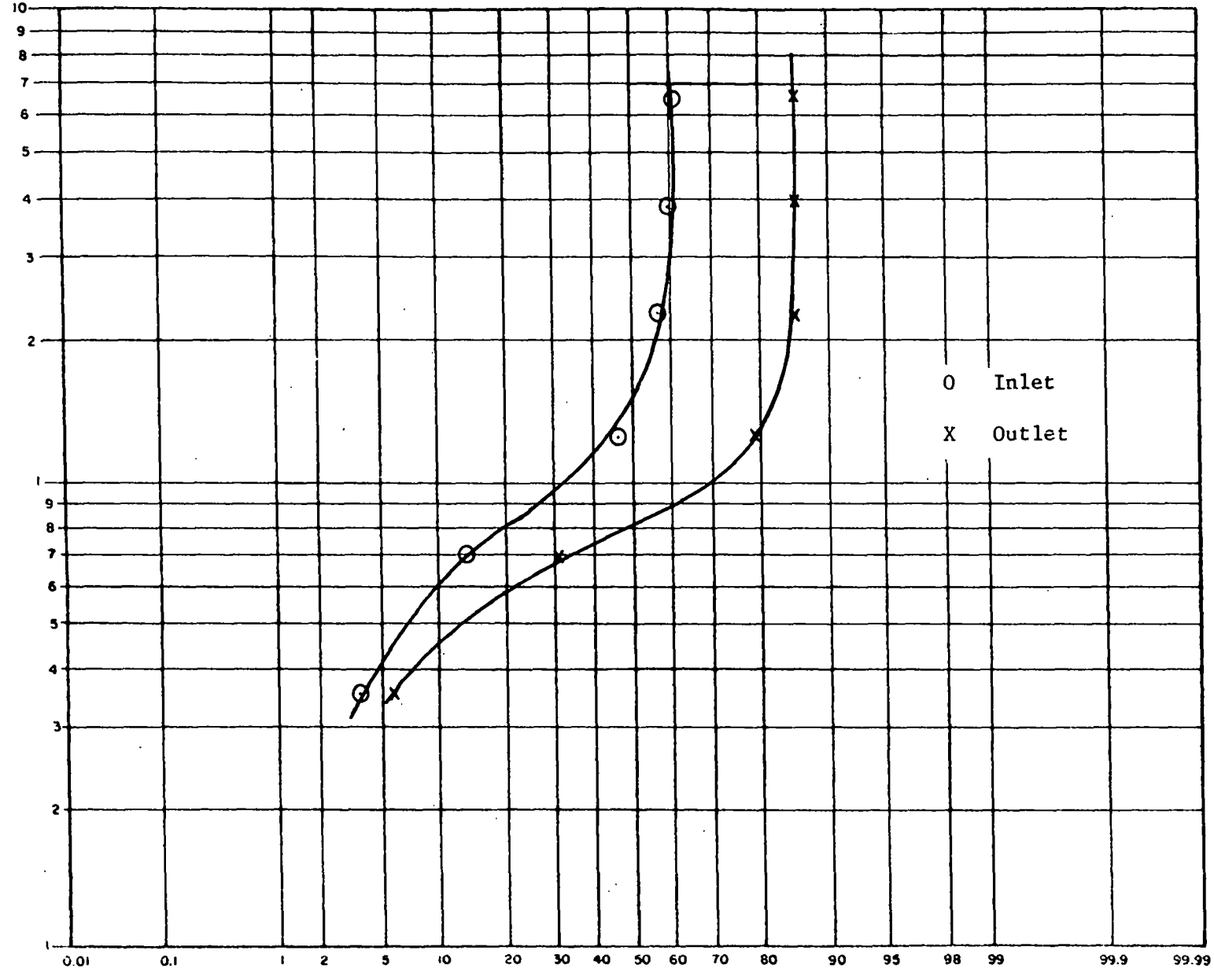

Figure 21. Particle Size Distribution(s) of Cyclone Undersize Dust for Test 18

cyclone with flyash and cupola dust, and served as the field calibration of the collection efficiency by particle size of the cyclone collectors as shown in Appendix B.

The particle size distributions of the cyclone undersize dust at the inlet and outlet show no clear trend. More often than not there is a significant shift in the size distribution but not in any consistant direction. For example, tests 2 and 4 were run at nearly identical conditions but the results showed opposite effects. Test 2 resulted in a substantially larger size at the outlet but test 4 resulted in a somewhat smaller size at the outlet. Tests 5, 6 and 7, on the other hand, resulted in practically no change between the inlet and outlet particle diameters but test 5 and 7 were run with sound and test 6 was run without sound.

A comparison of tests 8 and 9, however, indicates a positive influence of sound because of the larger size of the outlet cyclone undersize dust in test 8 with sound as compared to no change in test 9 without sound.

The lack of any clear trend of a change in the particle size of the cyclone undersize dust after going through the sonic agglomerator is also indicated in Figure 22. This is a plot of the mass median diameter of the fine particles at the inlet versus that at the outlet. Each point is numbered according to the test number in order to facilitate identifying each one with the system operating parameters in Table 1. As can be seen on Figure 22, test 2 resulted in the greatest increase in mass median diameter of the outlet dust. The reason for this is not understood and a repeat test at the same conditions (test 4) failed to demonstrate any increase in the outlet mass median diameter at all.

D. ESTIMATE OF OPERATING COSTS

An estimate of the operating costs was made for the Braxton sonic agglomerator. The operating parameters such as steam and water consumption and electrical requirements for each run were expanded to a 16.67 m^3/s (1000 m^3/min or 35,000 cfm) system by a simple multiplier. For example, if the system required 15 kilowatts at a flow rate of 2.2 m^3/s then 7.58 times 15 kilowatts, or 113.64 kilowatts, would be required for the scaled up unit. The same type of scaling was done for steam and water consumption and the

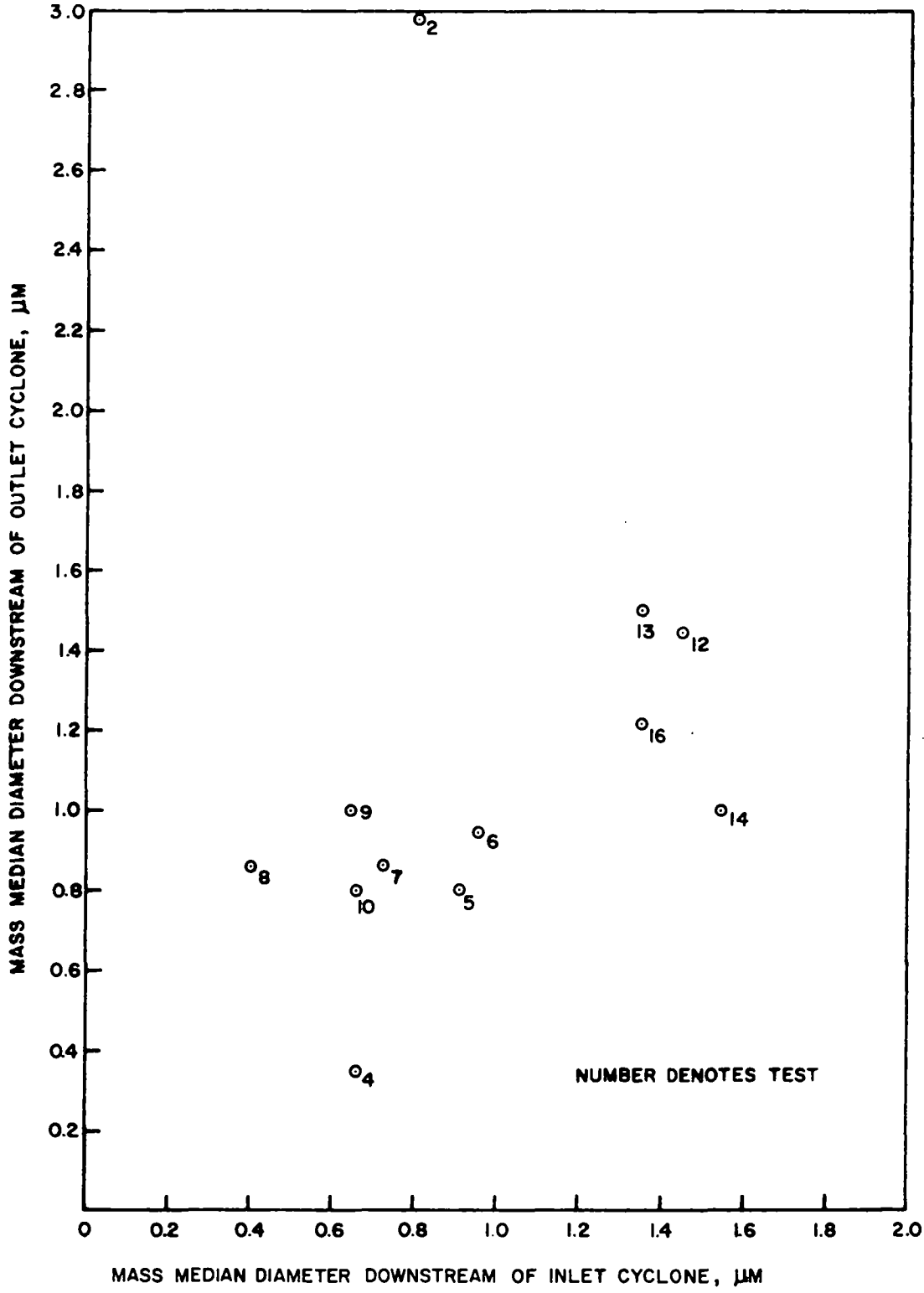

Figure 22. Effect of AVP System on Mass Median Diameters of Cyclone Undersize Dust.

cost for each parameter estimated for each test run in Table 4. An estimated annual operating cost based upon 8,000 hours operation is also included.

The estimated cost for steam consumption is based on a purchased price of $3.10 per 1,000 pounds. Water costs are based on $0.40 per 100 cubic feet and the electricity rates used are $0.025 per kilowatt hour.

It should be pointed out that the cost estimates in Table 4 do not include the additional power requirements for a high efficiency cyclone. Some of the earlier performance data were based on the use of the cyclone in the sampling train and the operating cost of a scaled up cyclone are not reflected in the cost estimates.

Test 7 reflects normal water and power consumption while test 8 shows the same conditions except for steam addition. The estimated annual operating cost under the conditions in test 7 is $13.30/$m^3$/minute ($0.38/cfm) and for test 8 it is $46.22/$m^3$/minute ($1.32/cfm). These estimates are based upon the previously explained conditions and costs but do not include any annualized capital costs.

It is clear that within the limitations of the assumptions and conditions associated with Table 4 that by far the most expensive item is steam. The effectiveness of steam addition is at best questionable and more than likely detrimental so it is safe to assume that the costs associated with steam use could be subtracted out.

Table 4. ESTIMATED OPERATING COSTS OF AVP SYSTEM[a]

Test	Cost per 1000 m^3 of Gas Treated, Dollars			Annual Cost, Dollars[e]
	Steam[b]	Water[c]	Electricity[d]	
1	0	0	0.0391	18,771
2	0	0.0056	0.0494	26,400
3	0	0.0056	0.0484	25,920
4	0	0.0056	0.0484	25,920
5	0	0.0028	0.0270	14,304
6	0	0.0028	0.0155	8,784
7	0	0.0028	0.0249	13,296
8	0.0688	0.0028	0.0247	46,224
9	0.0688	0.0028	0.0155	41,808
10	0.3440	0.0028	0.0243	178,128
12	0.0688	0	0.0290	46,944
13	0	0	0.0361	17,328
14	0.0688	0.0028	0.0418	54,432
16	0.2339	0	0.0299	126,624
18	0.0688	0.0028	0.0246	46,176
19	0.0688	0.0028	0.0254	46,560

[a] based on a 1000 m^3/min (35,000 cfm) system

[b] based on $3.10 per 1000 pounds

[c] based on $0.40 per 100 $ft.^3$

[d] based on $0.025 per kilowatt hour

[e] based on 8000 hours of operation per year

APPENDIX A

ACOUSTIC COAGULATION AND THE BRAXTON SONIC AGGLOMERATOR

Mednikov (1965) gave a much more advanced presentation on this subject than did Fuchs (1964) or Green and Lane (1964), and his results are applied here to the Braxton acoustic agglomerator. It is Mednikov's conclusion that for industrial gas cleaning situations, the predominant mechanism of acoustical agglomeration is the different vibratory velocities and phases of particles of different sizes, despite the great variety of possible mechanisms presented in the literature.

Coagulation is generally governed by the following equation:

$$dn/dt = -K\, n^2$$

where

t = time, sec

n = concentration, cm^{-3}

K = coagulation constant, cm^2 x cm/sec.

The units for K suggest the general mechanism: particles in motion "sweep" a given volume per unit time, the product of their effective cross sectional area and their velocity, and the number of particles is decreased by each effective particle-particle collision in this swept volume.

The aerodynamic diameter of a particle, or equivalently its "relaxation" time t, governs the particle's response to velocity changes of the medium in which it is suspended. The ratio of particle velocity amplitude Up to gas velocity amplitude Ug in a sonic field is (Fuchs, 1964; Mednikov, 1965):

$$Up/Ug \doteq 1/[\, 1 + (2\pi)^2\, (\tau/t_s)^2\,]^{\frac{1}{2}}$$

where

$\tau = C\rho_p\, d_p^{\,2}/18\, \mu$, the particle relaxation time, sec,

$t_s = 1/f$, the vibration period of the sound, sec,

f = sound frequency, sec^{-1} or Hz

d_p = particle diameter, cm,
ρ_p = particle density, g/cm^3,
μ = medium viscosity, poise

Roughly, this means that small particles, those having $2\pi\tau f \ll 1$, follow the gas vibrations, and large particles, those having $2\pi\tau f \gg 1$, do not vibrate appreciably. At the frequency of the Braxton device, ~ 400 Hz, the critical τ_c is

$$\tau_c = 1/2\pi f$$

$$\tau_c = 4.0 \times 10^{-4} \text{ sec}$$

which is the relaxation time of a 12-μm diameter particle of unit density. Particles of $\tau \ll \tau_c$ will agglomerate on particles of $\tau \gg \tau_c$, if they agglomerate at all. Since it takes many "small" particles to change the mass of a "large" particle, the primary change in the size distribution would be a decrease in the number (and mass) concentrations for particles having $\tau \ll \tau_c$ and an increase for particles having $\tau \gg \tau_c$, reflected by:

(a) a decrease in the total number concentration,
(b) an increase in the number mean and median diameters,
(c) no change in the mass mean diameter,
(d) an increase in the mass median diameter,
(e) a decrease in the geometric standard deviation (if a log-normal curve is fit).

Of all these effects, the most noticeable should be the change in the "small" particle concentration, here (Braxton) the respirable fraction. This may be the most useful test of whether or not the device is agglomerating particles.

Mednikov's model subdivides the aerosol into its small particle concentration n_2 and its large particle concentration n_1 (assumed to be constant with time). The coagulation equation for the aerosol becomes:

$$dn/dt \doteq dn_2/dt = - K_{a1} n_1 n_2$$

where

$n = n_1 + n_2$
K_{a1} = coagulation coefficient, cm^3/sec,

and

$$K_{a1} = 0\ (\overline{\pi r_1^2}\ U_g),$$

where

$\overline{\pi r_1^2}$ is an average cross-sectional area for the large particles and 0(x) means "of the order of magnitude of x."

The coagulation equation here becomes

$$n_2 \doteq (n_2)_o \exp\ (-\ K_{a1}\ n_1\ t)$$

and the exponential time dependence has been found in many experiments (Mednikov, 1965). Assuming $n_2 \gg n_1$, then $n \doteq n_2$ and $n_o \doteq (n_2)_o$.

Coagulation is appreciable, $n/n_o \ll 1$, if

$$Q = n_1\ r_1^2\ U_g t \gg 1.$$

The gas velocity amplitude is given by

$$U_g = (2J/\rho_g\ c_g)^{1/2}$$

where

J = sound intensity, erg/cm^2-sec, 10^{-7} W/cm^2,
ρ_g = gas density, g/cm^3,
c_g = gas speed of sound, cm/sec,
U_g = gas vibration velocity amplitude, cm/sec.

Coagulation will thus be improved by increasing

$$n_1\ \overline{r_1^2}\ J^{1/2}\ t_{res}$$

in the coagulation chamber; t_{res} is the residence time. Note the relatively weak dependence upon power level changes, $J^{1/2}$.

The Braxton device has a 5 hp acoustic power source radiating into a 3-foot diameter cylinder which is about 10 feet long. This gives a gas velocity amplitude:

$$U_g = \left[\frac{2x5 \text{ hp} \times 746 \text{ watts/hp} \times 10^7 \text{ erg/watt}}{1.2x10^{-3} \text{ g/cm}^3 \times 3.3x10^4 \text{ cm/sec} \times 6.3x10^3 \text{ cm}^2} \right]^{1/2} = 5.4x10^2 \text{ cm/sec.}$$

If the large particle concentration is due to the Braxton water spray nozzles, then that concentration is

$$n_1 = \dot{m}/(4\pi/3)\rho_w \overline{r^3} \dot{V}$$

where

$\dot{m}$ = mass flow of water, g/sec

$\dot{V}$ = volume flow of air, cm^3/sec

ρ_w = water density, g/cm^3

$\overline{r^3}$ = water droplet mass mean diameter, cm.

The residence time of the particles in the agglomerator chamber will be the chamber volume divided by the flow rate or

$$t_{res} = V_c/\dot{V} .$$

the parameter governing acoustic coagulation is

$$Q = n_1 \pi \overline{r_1^2} U_g t_{res}$$

and it will have a $\dot{V}^{-1}$ dependence on flow rate due to its residence time dependence; if the large particle concentration n_1 is due primarily to the water spray, as assumed, then $n_1 \propto \dot{V}^{-1}$ will increase the dependence of Q on $\dot{V}$ to $Q \propto \dot{V}^{-2}$. (This $\dot{V}^{-2}$ dependence of coagulation will be somewhat offset by increased large particle deposition at larger $\dot{V}$ due to impaction on walls and in bends and due to coagulation produced in non-oscillating accelerations of the air flow.) Since the spray concentration n_1 is related to the spray mass flow and mass average spray droplet radius $(\overline{r^3})^{1/3}$ by

$$\dot{m} \propto n \overline{r_1^3} \dot{V},$$

$$\dot{V} n_1 \overline{r_1^2} \propto \dot{m} (\overline{r_1^2}/\overline{r_1^3}),$$

$$(\overline{r_1^2}/\overline{r_1^3}) \sim 1/\overline{r_1} ,$$

the coagulation rate will be increased at constant droplet mass flow for smaller droplets, as long as they are large enough so their $\tau \gg \tau_c$.

Whether or not the spray evaporates completely can be estimated. The effect of a relative velocity $(U_p - U_g)$ between particle and fluid is to accelerate mass and heat transfer in comparison with the rates appropriate to a stationary particle. For water droplets evaporating, this multiplies the stationary mass loss rate by a ventilation factor (Green and Lane, 1964) of

$$\left[1 + 0.3\ (Re_p)^{1/2}\right]$$

where

$$Re_p = \rho\ (U_p - U_g)\ d_p/\mu\ .$$

For a falling 20-μm diameter water droplet $(U_p - U_g)$, $U_p = 1.2$ cm/sec and $Re_p = 1.6 \times 10^{-2}$, so that this ventilation factor is small. For acoustical $U_g = 5.4 \times 10^2$ cm/sec, and the Reynolds number becomes 7.3, so the evaporation rate is increased by about a factor of 1.8. At 80 percent r.h. and 20°C, a 20-μm diameter water droplet has a lifetime of 2.4 sec (Green and Lane, 1964); droplet lifetime is proportional to droplet area for droplets larger than 1 μm or so. The Braxton device has residence times $\lesssim$ 1 sec so that the droplets should not have evaporated completely before exiting the acoustic chamber.

An approximate calculation for the Braxton coagulation efficiency follows:

$\dot{V} \doteq 5{,}000$ cfm $= 200$ ft^3/sec
$V_c \doteq 100$ ft^3
} $t_{res} = 1.2$ sec

$J \doteq 5$ hp

$\overline{r_1} \doteq 10$ μm spray droplets $\doteq (\overline{r_1^3})^{1/3}$

$\dot{m} \doteq 1$ gal/min of spray

$\dot{m} \doteq 4$ liters/min $= 4 \times 10^3$ g/60 sec $= 0.66 \times 10^2$ g/sec

$$n_1\ \overline{r_1^2} \doteq \dot{m}/\dot{V}\ \overline{r_1}\ \rho_w$$

$U_g = 5.4 \times 10^2$ cm/sec

$\therefore Q = 3.14\ (2.8 \times 10^{-2}\ cm^{-1})(5.4 \times 10^2\ cm/sec)(1.2\ sec)$

$Q = 57$

$Q \gg 1$ so $n_2/(n_2)_o \ll 1$ and thus Braxton device should be efficient in reducing the small particles by droplet-particle collision.

(This kind of calculation can only tell whether $n/n_o \ll 1$ or not and should not be taken as a means for getting $n/n_o = \exp(-Q)$ more accurately than to an order of magnitude in Q. There are many second-order effects.)

A somewhat more sophisticated calculation of the acoustic agglomeration would take into account the tendency of the sub-micron fraction of the aerosol to avoid capture by following the streamlines of flow around the larger droplets as the flow oscillates. This can be added to the model through an efficiency factor ϵ multiplying Q, acknowledging that the geometric cross-section of the large particles, $\pi \overline{r_1^2}$, is different from the effective collision cross-section, $\epsilon\ \pi\ \overline{r_1^2}$. This factor ϵ will be a function of the aerodynamic diameter of the small particles, or $\epsilon = \epsilon(r_2)$. Theory and practice indicate that $\epsilon \sim 1$ for $\tau_2\ U_g/r_1 \gg 1$ and $\epsilon \to 0$ for $\tau_2\ U_g/r_1 \ll 1$. For $r_1 \doteq 10\ \mu m$, $U_g \doteq 6 \times 10^2$ cm/sec, $\tau_2\ U_g/r_1 = 1$ at $\tau_2 = 1.7 \times 10^{-6}$ sec, which corresponds to $d_2 = 2\ r_2 \doteq 0.7\ \mu m$. Thus we would expect the agglomerator to be significantly less efficient for particles smaller than 1/2-μm diameter.

REFERENCES

Fuchs, N.A. (1964): Mechanics of Aerosols, Pergamon Press, New York.

Green, H.L. and Lane, W.R. (1964): Particulate Clouds: Dusts, Smokes and Mists.

Mednikov, E.P (1963): Translator: Larrick, C.V., Acoustic Coagulation and Precipitation of Aerosols, Consultants Bureau, New York, 1965.

APPENDIX B

CALIBRATION OF SAMPLING EQUIPMENT

Cyclone Calibration:

The cyclones were calibrated in the GCA laboratory using a calibrated orifice to determine the flow rate. The pressure drop across the cyclone was plotted against the flow rate through the orifice on log-log paper and the line of best fit drawn. The resulting calibration curves are presented in Figures B-1 through B-4.

Critical Orifice Flow Rate Determination:

The critical flow rates through the orifices were determined using a Schutte and Koerting calibrated rotameter. The measured flow rates corrected to standard conditions are presented in Table B-1.

Table B-1. Critical Orifice Flow Rates

Orifice	Flow Rate at Standard Conditions, scfm
A	0.965
B	1.060

Cyclone Removal Efficiency by Particle Size

Field tests 15 and 17 were run to determine the cyclone removal efficiency by particle size for fly ash and cupola dust. Andersen impactors were located upstream and downstream of the sample train cyclone. The samples were collected from the inlet sampling port of the Braxton AVP system. System parameters are presented in Table B-2.

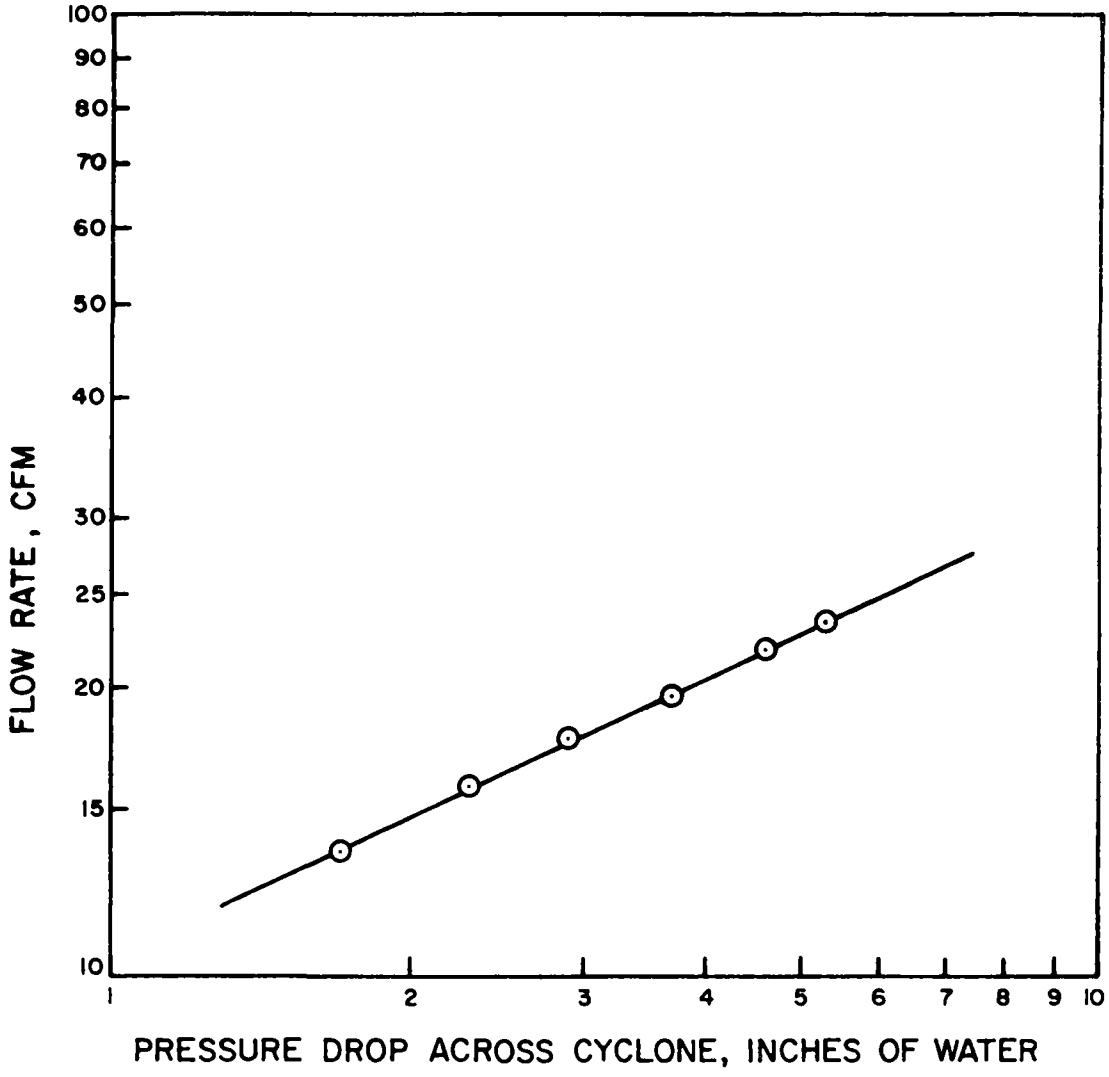

Figure B-1. Cyclone #1 Curve

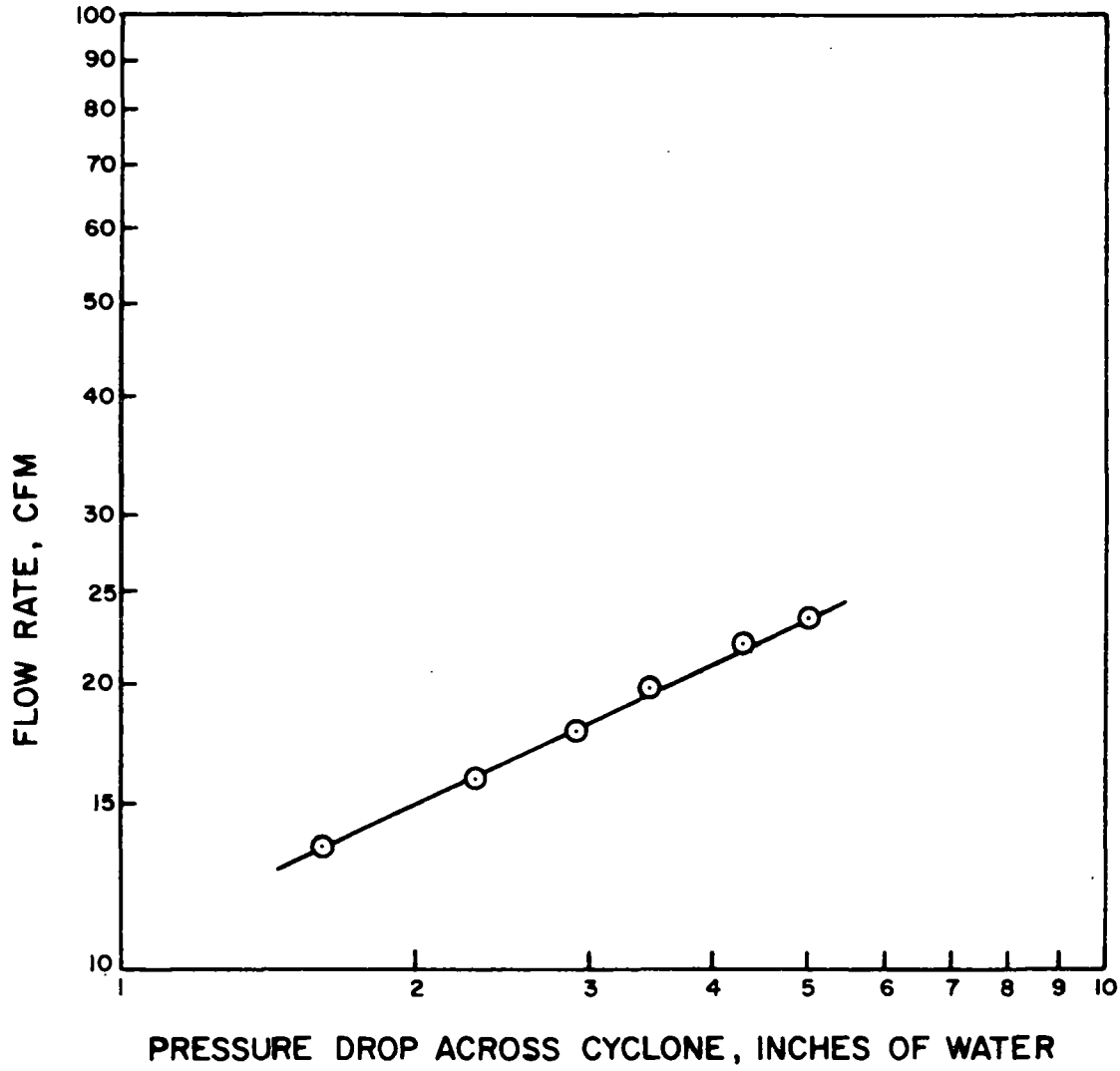

Figure B-2. Cyclone #2 Calibration Curve

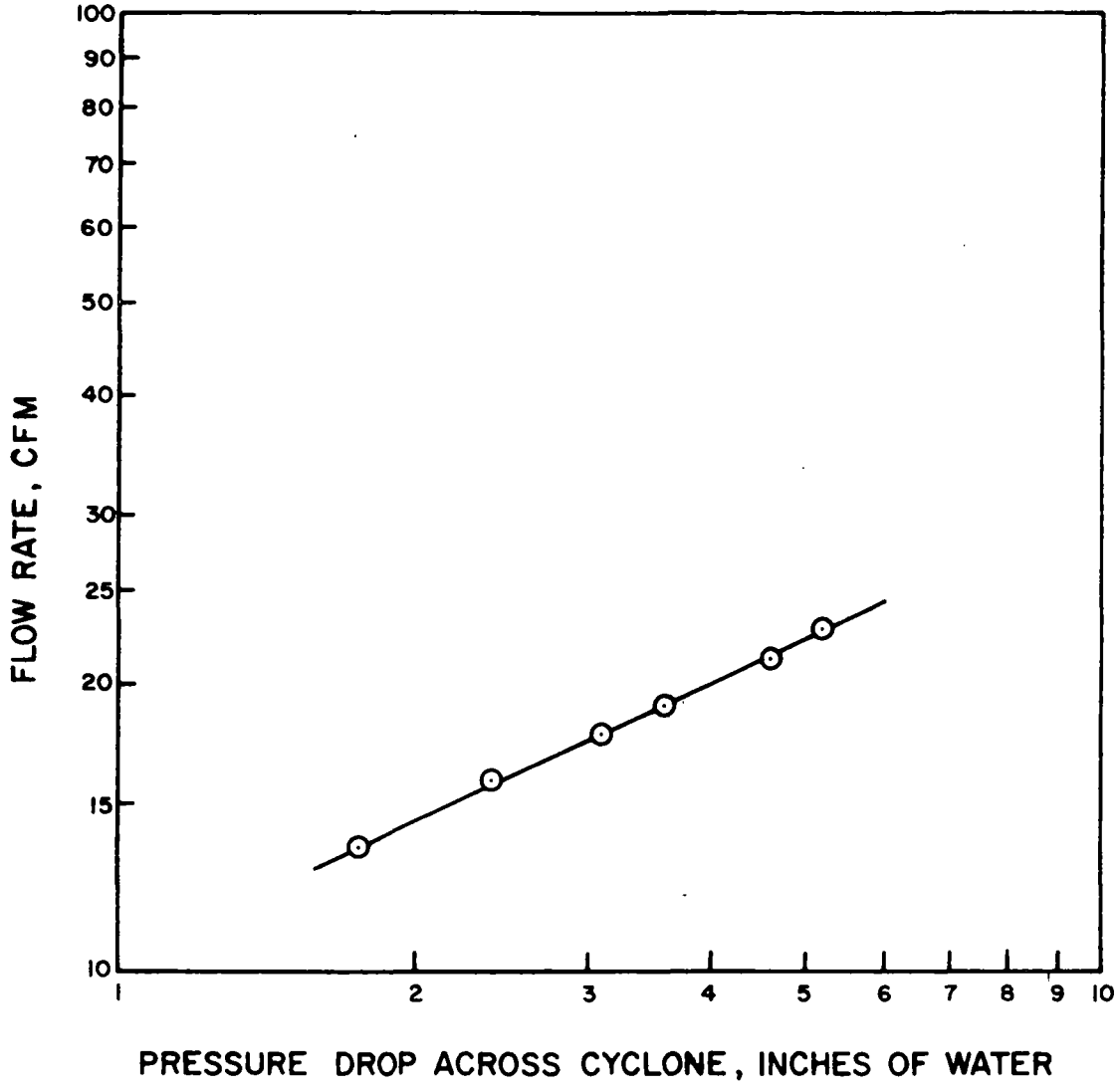

Figure B-3. Cyclone #3 Calibration Curve

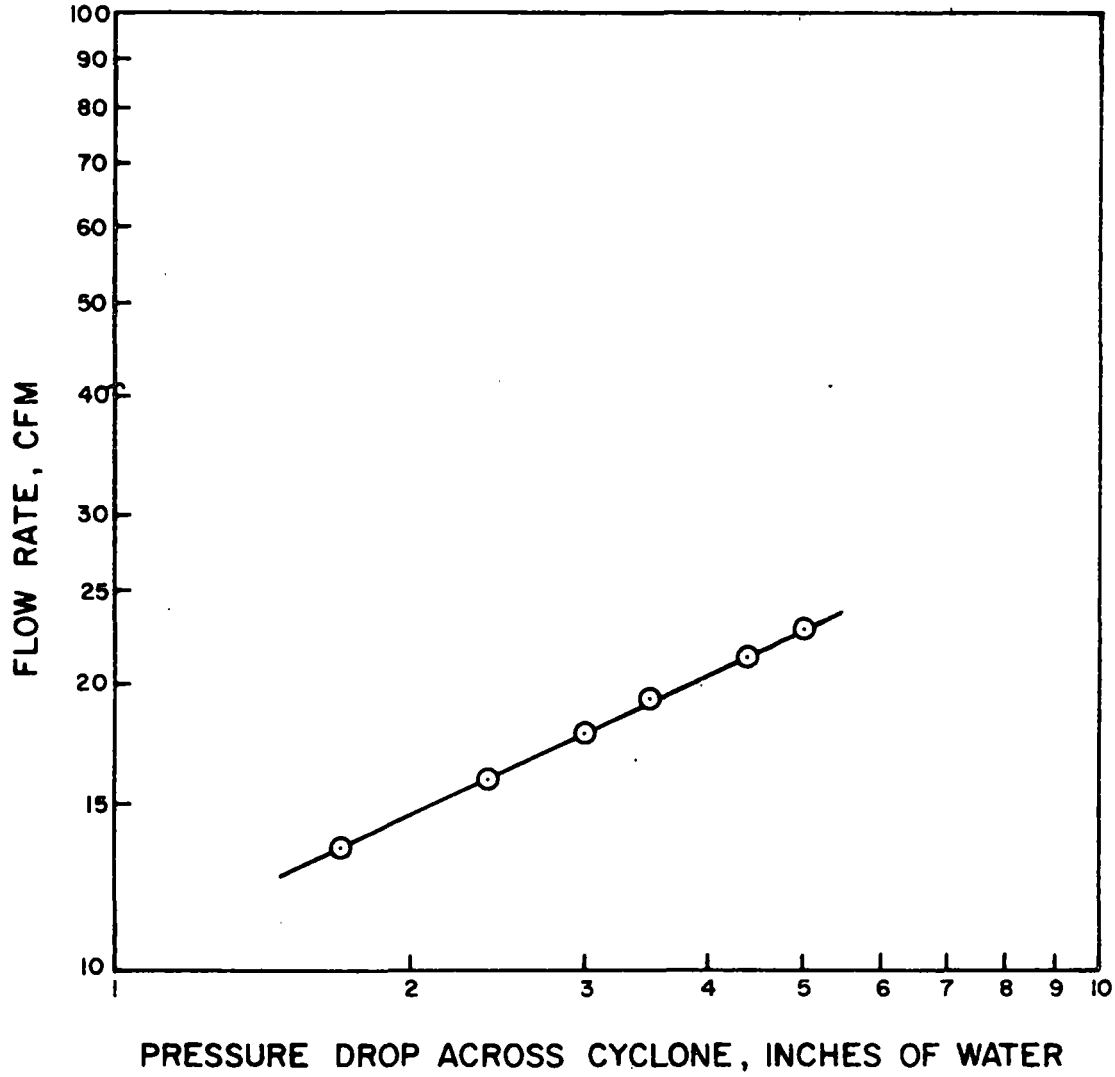

Figure B-4. Cyclone #4 Calibration Curve

Table B-2. System Parameters During Cyclone Removal Efficiency Tests

TEST #	DUST TYPE	SYSTEM FLOW, m^3/s	CONCENTRATION, g/m^3	DUST PRECONDITIONING
15	fly ash	2.5 (5000 cfm)	2.80 (1.22 gr/ft^3)	none
17	cupola	2.5 (5000 cfm)	3.06 (1.34 gr/ft^3)	none

Results of cyclone removal efficiency measurements for fly ash and cupola dust are presented in Figures B-5 and B-6. Difficulties encountered necessitated combining the mass collected on certain impactor stages. In the fly ash test, removal efficiencies were determined for the combined first and second stage and for the combined fourth, fifth and sixth stages. Combining was required for the first and second stage because of reintrainment which resulted from the collection of too-large a sample. Combining of stages 4, 5 and six was used to compensate for the clogging of several of the jets which impact on stage 5. In the cupola dust test, removal efficiencies were also calculated for the combined fourth, fifth and sixth stages due to clogging of the jets which impact on stage 5.

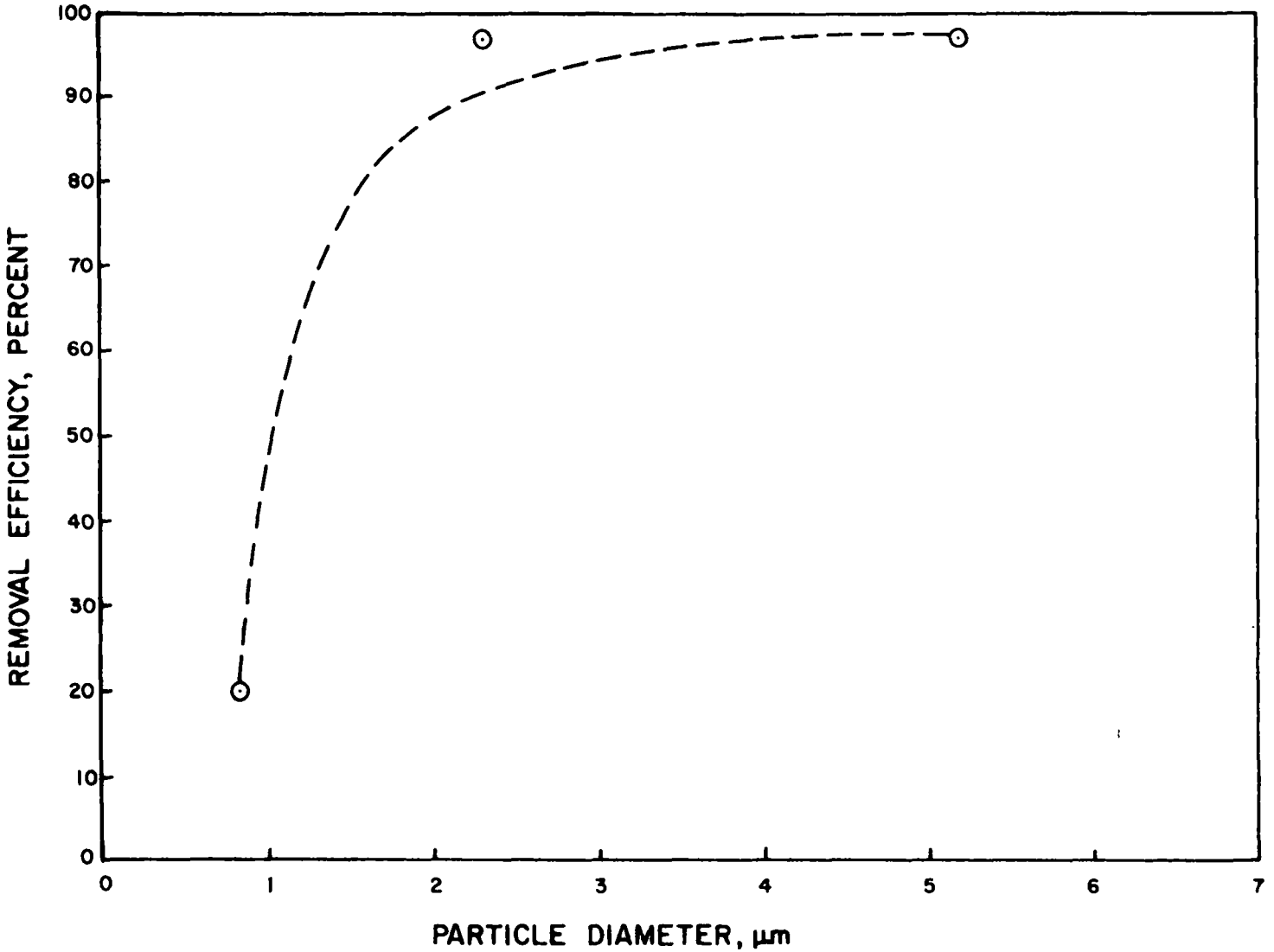

Figure B-5. Cyclone Removal Efficiency by Particle Size of Fly Ash

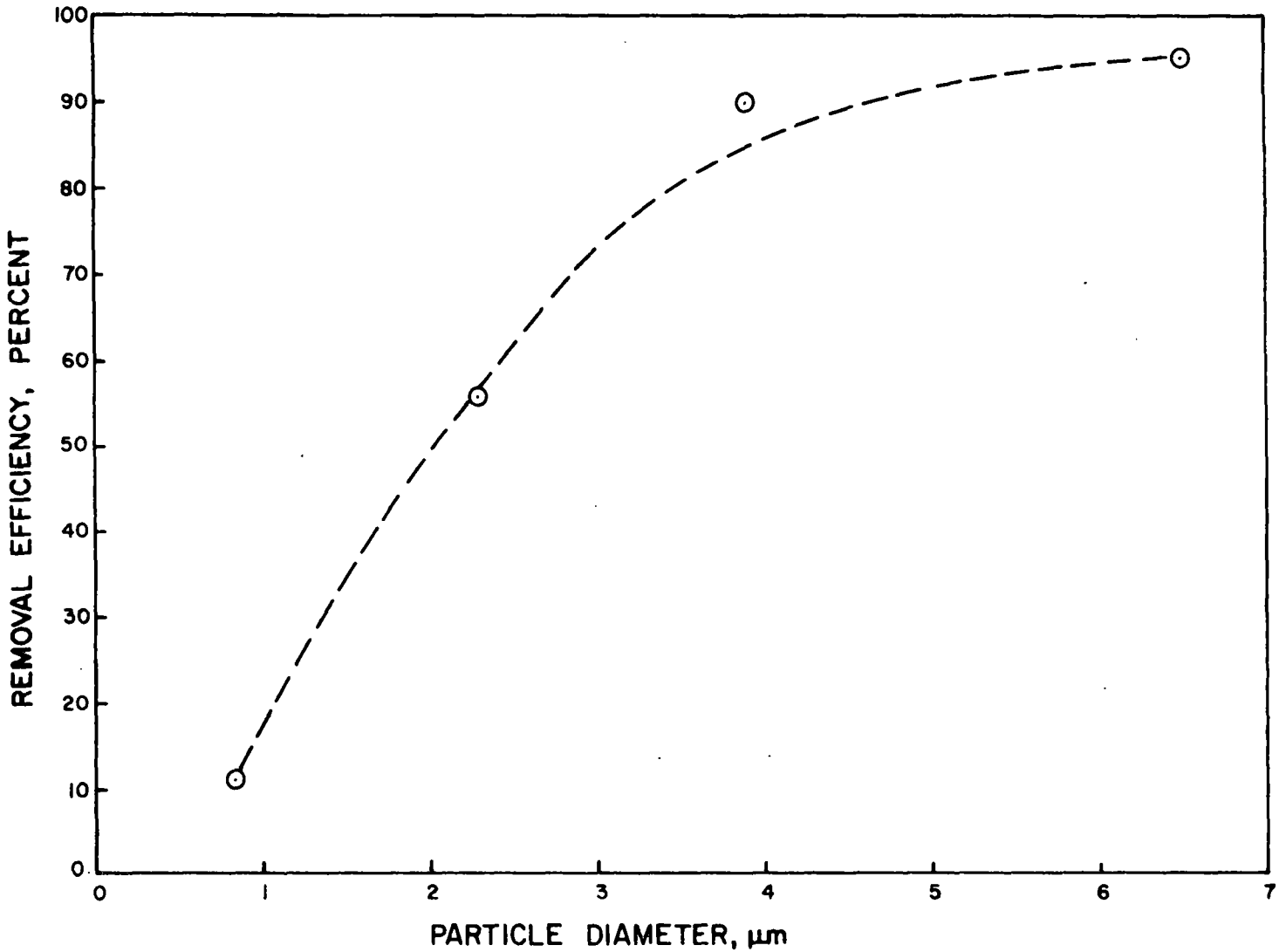

Figure B-6. Cyclone Removal Efficiency by Particle Size of Cupola Dust

APPENDIX C

PARTICLE SIZE DISTRIBUTION DATA

The following table presents the particle size distribution data as determined by six stage Andersen impactors. Before use, the collection surfaces were coated with a thin, uniform layer of petroleum jelly to minimize particle bounce and reintrainment.

The aerodynamic particle size cutoff for each stage is based upon an assumed particle density of 2.0. Although this value is only an estimate, any shift in the size cutoff due to a different density would be exactly the same for both upstream and downstream impactors.

Table C-1. PARTICLE SIZE DISTRIBUTION DATA

TEST 1

OUTLET

Stage	Size Range, μm	Cumulative Mass, Percent
Filter	< 0.36	0.0
6	> 0.36 - < 0.7	17.7
5	> 0.7 - < 1.4	40.8
4	> 1.4 - < 2.3	56.9
3	> 2.3 - < 3.9	57.7
2	> 3.9 - < 6.5	75.4
1	> 6.5	100.0

TEST 2

INLET

Stage	Size Range, μm	Cumulative Mass, Percent
Filter	< 0.36	0.0
6	> 0.36 - < 0.7	42.9
5	> 0.7 - < 1.4	70.1
4	> 1.4 - < 2.3	70.1
3	> 2.3 - < 3.9	79.2
2	> 3.9 - < 6.5	87.0
1	> 6.5	100.0

OUTLET

Stage	Size Range, μm	Cumulative Mass, Percent
Filter	< 0.36	0.8
6	> 0.36 - < 0.7	34.2
5	> 0.7 - < 1.4	40.8
4	> 1.4 - < 2.3	46.7
3	> 2.3 - < 3.9	55.8
2	> 3.9 - < 6.5	89.2
1	> 6.5	100.0

Table C-1 (continued). PARTICLE SIZE DISTRIBUTION DATA

TEST 3

OUTLET

Stage	Size Range, μm	Cumulative Mass, Percent
Filter	< 0.36	15.4
6	> 0.36 - < 0.7	48.1
5	> 0.7 - < 1.4	59.6
4	> 1.4 - < 2.3	63.5
3	> 2.3 - < 3.9	67.3
2	> 3.9 - < 6.5	69.2
1	> 6.5	100.0

TEST 4

INLET

Stage	Size Range, μm	Cumulative Mass, Percent
Filter	< 0.36	29.0
6	> 0.36 - < 0.7	52.2
5	> 0.7 - < 1.4	68.0
4	> 1.4 - < 2.3	71.3
3	> 2.3 - < 3.9	72.4
2	> 3.9 - < 6.5	72.4
1	> 6.5	100.0

OUTLET

Stage	Size Range, μm	Cumulative Mass, Percent
Filter	< 0.36	42.8
6	> 0.36 - < 0.7	79.5
5	> 0.7 - < 1.4	91.6
4	> 1.4 - < 2.3	92.4
3	> 2.3 - < 3.9	93.5
2	> 3.9 - < 6.5	93.5
1	> 6.5	100.0

Table C-1 (continued). PARTICLE SIZE DISTRIBUTION DATA

TEST 5

INLET			OUTLET		
Stage	Size Range, μm	Cumulative Mass, Percent	Stage	Size Range, μm	Cumulative Mass, Percent
Filter	< 0.36	21.4	Filter	< 0.36	16.1
6	> 0.36 - < 0.7	41.9	6	> 0.36 - < 0.7	43.9
5	> 0.7 - < 1.4	62.0	5	> 0.7 - < 1.4	71.1
4	> 1.4 - < 2.3	67.1	4	> 1.4 - < 2.3	79.4
3	> 2.3 - < 3.9	70.7	3	> 2.3 - < 3.9	80.5
2	> 3.9 - < 6.5	73.7	2	> 3.9 - < 6.5	81.9
1	> 6.5	100.0	1	> 6.5	100.0

TEST 6

INLET			OUTLET		
Stage	Size Range, μm	Cumulative Mass, Percent	Stage	Size Range, μm	Cumulative Mass, Percent
Filter	< 0.36	20.9	Filter	< 0.36	17.2
6	> 0.36 - < 0.7	40.2	6	> 0.36 - < 0.7	37.0
5	> 0.7 - < 1.4	60.4	5	> 0.7 - < 1.4	62.4
4	> 1.4 - < 2.3	67.8	4	> 1.4 - < 2.3	69.3
3	> 2.3 - < 3.9	78.8	3	> 2.3 - < 3.9	69.5
2	> 3.9 - < 6.5	82.6	2	> 3.9 - < 6.5	70.7
1	> 6.5	100.0	1	> 6.5	100.0

Table C-1 (continued). PARTICLE SIZE DISTRIBUTION DATA

TEST 7

INLET			OUTLET		
Stage	Size Range, μm	Cumulative Mass, Percent	Stage	Size Range, μm	Cumulative Mass, Percent
Filter	< 0.36	25.6	Filter	< 0.36	18.3
6	> 0.36 - < 0.7	50.4	6	> 0.36 - < 0.7	42.0
5	> 0.7 - < 1.4	68.4	5	> 0.7 - < 1.4	65.7
4	> 1.4 - < 2.3	71.8	4	> 1.4 - < 2.3	72.4
3	> 2.3 - < 3.9	71.8	3	> 2.3 - < 3.9	74.6
2	> 3.9 - < 6.5	71.8	2	> 3.9 - < 6.5	76.8
1	> 6.5	100.0	1	> 6.5	100.0

TEST 8

INLET			OUTLET		
Stage	Size Range, μm	Cumulative Mass, Percent	Stage	Size Range, μm	Cumulative Mass, Percent
Filter	< 0.36	43.6	Filter	< 0.36	6.7
6	> 0.36 - < 0.7	81.6	6	> 0.36 - < 0.7	34.7
5	> 0.7 - < 1.4	95.1	5	> 0.7 - < 1.4	85.4
4	> 1.4 - < 2.3	95.1	4	> 1.4 - < 2.3	85.7
3	> 2.3 - < 3.9	95.1	3	> 2.3 - < 3.9	86.1
2	> 3.9 - < 6.5	95.1	2	> 3.9 - < 6.5	86.4
1	> 6.5	100.0	1	> 6.5	100.0

Table C-1 (continued). PARTICLE SIZE DISTRIBUTION DATA

TEST 9

INLET			OUTLET		
Stage	Size Range, μm	Cumulative Mass, Percent	Stage	Size Range, μm	Cumulative Mass, Percent
Filter	< 0.36	27.6	Filter	< 0.36	11.4
6	> 0.36 - < 0.7	55.1	6	> 0.36 - < 0.7	27.2
5	> 0.7 - < 1.4	88.2	5	> 0.7 - < 1.4	91.2
4	> 1.4 - < 2.3	88.2	4	> 1.4 - < 2.3	92.1
3	> 2.3 - < 3.9	88.2	3	> 2.3 - < 3.9	94.8
2	> 3.9 - < 6.5	88.2	2	> 3.9 - < 6.5	95.7
1	> 6.5	100.0	1	> 6.5	100.0

TEST 10

INLET			OUTLET		
Stage	Size Range, μm	Cumulative Mass, Percent	Stage	Size Range, μm	Cumulative Mass, Percent
Filter	< 0.36	18.3	Filter	< 0.36	10.2
6	> 0.36 - < 0.7	50.6	6	> 0.36 - < 0.7	40.7
5	> 0.7 - < 1.4	76.6	5	> 0.7 - < 1.4	81.0
4	> 1.4 - < 2.3	78.6	4	> 1.4 - < 2.3	86.9
3	> 2.3 - < 3.9	78.6	3	> 2.3 - < 3.9	86.9
2	> 3.9 - < 6.5	78.6	2	> 3.9 - < 6.5	86.9
1	> 6.5	100.0	1	> 6.5	100.0

Table C-1 (continued). PARTICLE SIZE DISTRIBUTION DATA

TEST 12

INLET			OUTLET		
Stage	Size Range, μm	Cumulative Mass, Percent	Stage	Size Range, μm	Cumulative Mass, Percent
Filter	< 0.36	10.7	Filter	< 0.36	3.1
6	> 0.36 - < 0.7	27.5	6	> 0.36 - < 0.7	14.0
5	> 0.7 - < 1.4	48.9	5	> 0.7 - < 1.4	47.0
4	> 1.4 - < 2.3	55.2	4	> 1.4 - < 2.3	69.3
3	> 2.3 - < 3.9	57.2	3	> 2.3 - < 3.9	71.5
2	> 3.9 - < 6.5	58.8	2	> 3.9 - < 6.5	71.9
1	> 6.5	100.0	1	> 6.5	100.0

TEST 13

INLET			OUTLET		
Stage	Size Range, μm	Cumulative Mass, Percent	Stage	Size Range, μm	Cumulative Mass, Percent
Filter	< 0.36	4.1	Filter	< 0.36	1.6
6	> 0.36 - < 0.7	16.9	6	> 0.36 - < 0.7	17.2
5	> 0.7 - < 1.4	51.1	5	> 0.7 - < 1.4	39.2
4	> 1.4 - < 2.3	57.2	4	> 1.4 - < 2.3	51.8
3	> 2.3 - < 3.9	60.3	3	> 2.3 - < 3.9	54.4
2	> 3.9 - < 6.5	63.2	2	> 3.9 - < 6.5	56.3
1	> 6.5	100.0	1	> 6.5	100.0

Table C-1 (continued). PARTICLE SIZE DISTRIBUTION DATA

TEST 14

INLET			OUTLET		
Stage	Size Range, μm	Cumulative Mass, Percent	Stage	Size Range, μm	Cumulative Mass, Percent
Filter	< 0.36	4.6	Filter	< 0.36	0.0
6	> 0.36 - < 0.7	20.1	6	> 0.36 - < 0.7	18.6
5	> 0.7 - < 1.4	53.6	5	> 0.7 - < 1.4	69.2
4	> 1.4 - < 2.3	70.6	4	> 1.4 - < 2.3	85.5
3	> 2.3 - < 3.9	81.4	3	> 2.3 - < 3.9	88.4
2	> 3.9 - < 6.5	86.6	2	> 3.9 - < 6.5	88.4
1	> 6.5	100.0	1	> 6.5	100.0

TEST 15

BEFORE CYCLONE			AFTER CYCLONE		
Stage	Size Range, μm	Cumulative Mass, Percent	Stage	Size Range, μm	Cumulative Mass, Percent
Filter	< 0.36	0.0	Filter	< 0.36	1.2
6	> 0.36 - < 0.7	1.4	6	> 0.36 - < 0.7	17.2
5	> 0.7 - < 1.4	3.6	5	> 0.7 - < 1.4	59.3
4	> 1.4 - < 2.3	6.5	4	> 1.4 - < 2.3	66.0
3	> 2.3 - < 3.9	13.5	3	> 2.3 - < 3.9	68.6
2	> 3.9 - < 6.5	53.5	2	> 3.9 - < 6.5	70.9
1	> 6.5	100.0	1	> 6.5	100.0

Table C-1 (continued). PARTICLE SIZE DISTRIBUTION DATA

TEST 16

INLET			OUTLET		
Stage	Size Range, μm	Cumulative Mass, Percent	Stage	Size Range, μm	Cumulative Mass, Percent
Filter	< 0.36	4.4	Filter	< 0.36	0.0
6	> 0.36 - < 0.7	24.4	6	> 0.36 - < 0.7	28.1
5	> 0.7 - < 1.4	62.9	5	> 0.7 - < 1.4	65.6
4	> 1.4 - < 2.3	79.2	4	> 1.4 - < 2.3	71.9
3	> 2.3 - < 3.9	85.9	3	> 2.3 - < 3.9	71.9
2	> 3.9 - < 6.5	89.6	2	> 3.9 - < 6.5	73.5
1	> 6.5	100.0	1	> 6.5	100.0

TEST 17

BEFORE CYCLONE			AFTER CYCLONE		
Stage	Size Range, μm	Cumulative Mass, Percent	Stage	Size Range, μm	Cumulative Mass, Percent
Filter	< 0.36	0.0	Filter	< 0.36	2.1
6	> 0.36 - < 0.7	3.7	6	> 0.36 - < 0.7	20.5
5	> 0.7 - < 1.4	8.0	5	> 0.7 - < 1.4	56.2
4	> 1.4 - < 2.3	12.0	4	> 1.4 - < 2.3	64.4
3	> 2.3 - < 3.9	15.0	3	> 2.3 - < 3.9	71.4
2	> 3.9 - < 6.5	25.3	2	> 3.9 - < 6.5	77.6
1	> 6.5	100.0	1	> 6.5	100.0

Table C-1 (continued). PARTICLE SIZE DISTRIBUTION DATA

TEST 18

INLET			OUTLET		
Stage	Size Range, μm	Cumulative Mass, Percent	Stage	Size Range, μm	Cumulative Mass, Percent
Filter	< 0.36	2.5	Filter	< 0.36	5.7
6	> 0.36 - < 0.7	13.1	6	> 0.36 - < 0.7	31.1
5	> 0.7 - < 1.4	44.9	5	> 0.7 - < 1.4	79.0
4	> 1.4 - < 2.3	55.5	4	> 1.4 - < 2.3	84.3
3	> 2.3 - < 3.9	59.4	3	> 2.3 - < 3.9	84.3
2	> 3.9 - < 6.5	61.4	2	> 3.9 - < 6.5	84.3
1	> 6.5	100.0	1	> 6.5	100.0

APPENDIX D

LABORATORY SIZING OF TEST DUSTS

The test dusts used in the field program were first dispersed in the laboratory and their particle size distribution determined with Andersen cascade impactors. The results are shown in Tables D-1 and D-2 and Figures D-1 and D-2.

The dusts were dispersed with an air ejector similar to the one used in the Braxton dust feed system except the compressed air supplied to the laboratory system was considerably higher (90 psi) then that supplied to the field system (20 psi). This probably led to more nearly complete breakup of the agglomerates in the bulk dust and hence an aerosol of smaller particle size than was achieved in the Braxton dust dispersion system.

As expected the cupola dust displayed a much smaller particle size distribution than the fly ash. Under the laboratory dispersion conditions the mass median diameter of the cupola dust was about 1.1 micrometers and the mass median diameter of the fly ash was about 9 micrometers.

Table D-1. Particle Size Distribution for Laboratory Dispersed Cupola Dust

Stage	Size Range, μm	Cumulative Mass, Percent
Filter	<0.36	16.2
6	>0.36 - <0.7	32.3
5	>0.7 - <1.4	54.5
4	>1.4 - <2.3	54.5
3	>2.3 - <3.9	54.5
2	>3.9 - <6.5	54.5
1	>6.5	100.0

Table D-2. Particle Size Distribution for Laboratory Dispersed Fly Ash

Stage	Size Range, μm	Cumulative Mass, Percent
Filter	<0.36	1.8
6	>0.36 - <0.7	3.2
5	>0.7 - <1.4	6.8
4	>1.4 - <2.3	12.2
3	>2.3 - <3.9	20.7
2	>3.9 - <6.5	36.5
1	>6.5	100.0

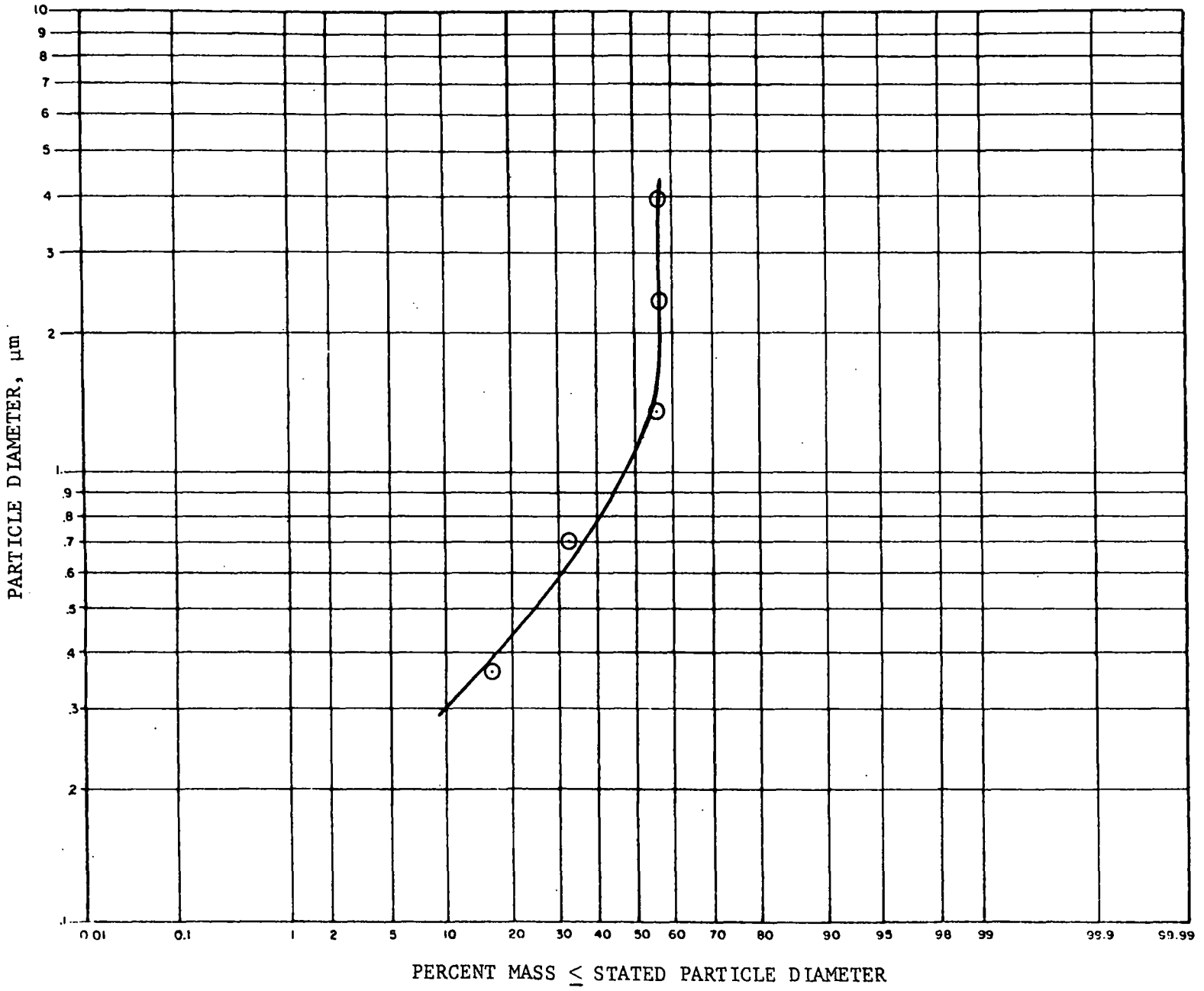

Figure D-1. Particle Size Distribution for Laboratory Dispersed Cupola Dust

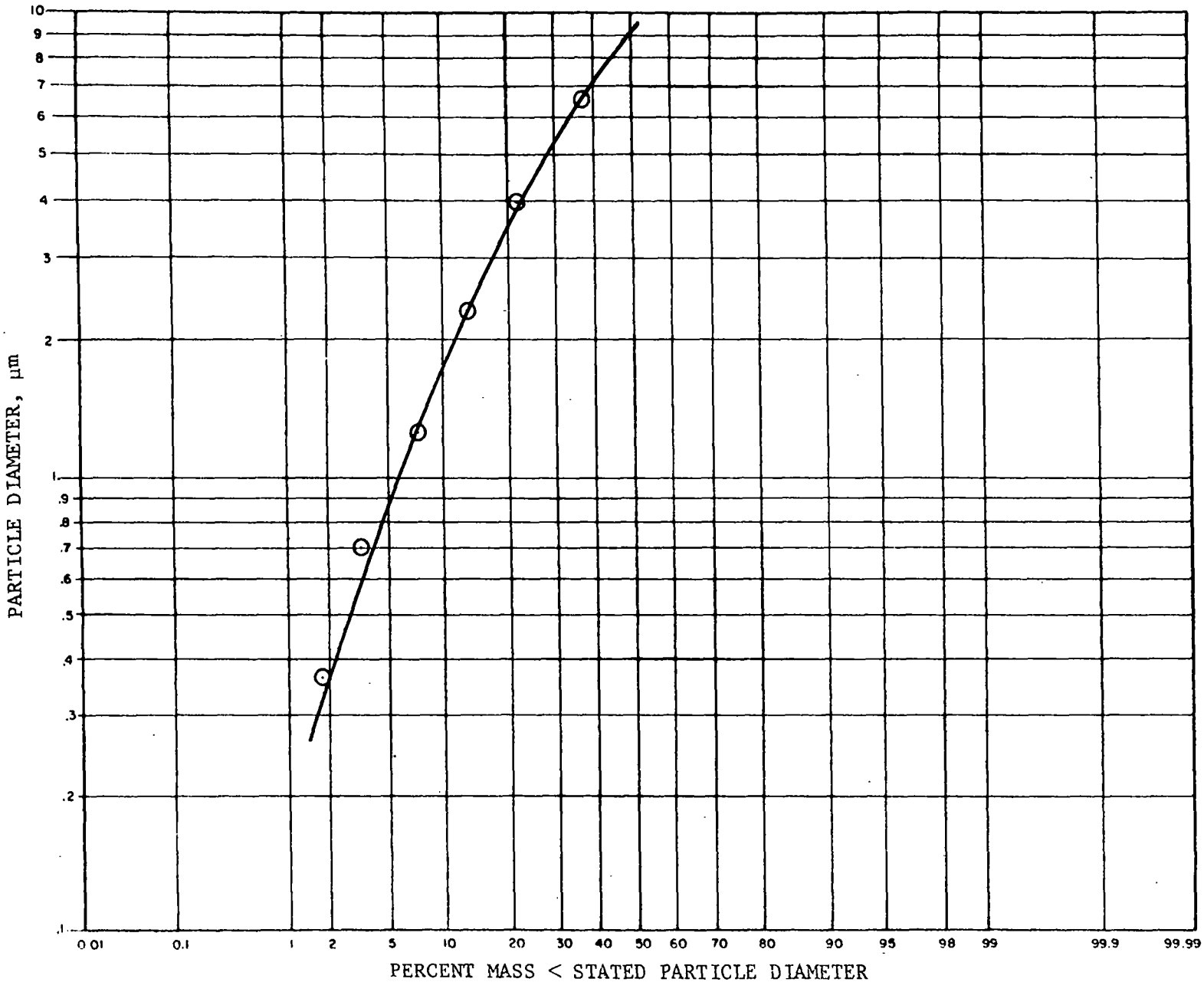

Figure D-2. Particle Size Distribution for Laboratory Dispersed Fly Ash

TECHNICAL REPORT DATA
(Please read Instructions on the reverse before completing)

1. REPORT NO.	2.	3. RECIPIENT'S ACCESSION NO.
EPA-650/2-74-036		

4. TITLE AND SUBTITLE	5. REPORT DATE
Braxton Sonic Agglomerator Evaluation	May 1974
	6. PERFORMING ORGANIZATION CODE

7. AUTHOR(S)	8. PERFORMING ORGANIZATION REPORT NO.
Richard Dennis, Robert Bradway, and Reed Cass	

9. PERFORMING ORGANIZATION NAME AND ADDRESS	10. PROGRAM ELEMENT NO.
GCA Corporation GCA/Technology Division Bedford, Massachusetts 01730	1AB012; ROAP 21ADL-04
	11. CONTRACT/GRANT NO.
	68-02-1316 (Task 1)

12. SPONSORING AGENCY NAME AND ADDRESS	13. TYPE OF REPORT AND PERIOD COVERED
EPA, Office of Research and Development NERC-RTP, Control Systems Laboratory Research Triangle Park, NC 27711	Final
	14. SPONSORING AGENCY CODE

15. SUPPLEMENTARY NOTES

16. ABSTRACT The report is an evaluation of a novel air pollution control system developed by the Braxton Corporation. The alternating velocity precipitator, or sonic agglomerator, is designed to decrease the number and increase the size of particles in a gas stream by agglomeration induced by a standing sound wave through which the aerosol moves. A prototype alternating velocity precipitator was tested to determine its basic performance characteristics and to evaluate the effect of adding water and/or steam to the systems performance. Tests indicate that the device decreases the mass of fine particles but that the reduction is more highly correlated to the use of water sprays than to the use of the sonic generator. The correlation coefficients relating the use of sound and water sprays to fine particle reduction, however, were not statistically significant. The particle size distributions of the fine particles at both the inlet and outlet of the sonic agglomerator were determined with Andersen cascade impactors. Although shifts between the inlet and outlet size distributions were often observed, there was no clear trend to the changes and they could not be correlated to system operating parameters.

17. KEY WORDS AND DOCUMENT ANALYSIS

a. DESCRIPTORS	b. IDENTIFIERS/OPEN ENDED TERMS	c. COSATI Field/Group
Air Pollution	Air Pollution Control	13B
Aerosols	Stationary Sources	20A
Acoustics	Braxton Sonic Agglomerator	7A
Sound Waves		7D
Precipitators	Alternating Velocity Precipitator	
Agglomeration		
Particle Size		
Particle Size Distribution		
Gas Flow	Particulates	20D

18. DISTRIBUTION STATEMENT	19. SECURITY CLASS *(This Report)*	21. NO. OF PAGES
Unlimited	Unclassified	
	20. SECURITY CLASS *(This page)*	22. PRICE
	Unclassified	

EPA Form 2220-1 (9-73)